# 西南林业大学博士研究生招生
# “申请-审核制”审核材料

申请人姓名：倪鸣源

申 请 导 师：栗忠飞

申 请 专 业：（090707）水土保持与荒漠化防治

申 请 学 院：（002）生态与环境学院

考 生 类 别：往届毕业生

申 请 年 度：2024

4、 外语能力证书

# 全国大学英语四级考试
## 成绩报告单

CET®

姓　　名：倪鸣源

学　　校：广西师范大学

院（系）：生命科学学院

准考证号：[redacted]

身份证号：[redacted]

考试时间：2015 年 12 月

**总分：** 441　具备英语四级口试报考资格

| 听力 (35%) | 阅读 (35%) | 写作和翻译 (30%) |
|---|---|---|
| 129 | 174 | 138 |

成绩单编号：152145108004527

教育部考试中心

证书专用章

# 5、 学术能力证明材料



given conductivity, the deciduous tree species exhibited stronger vessel wall reinforcement (safety) than the evergreen tree species, which might be due to the fact that evergreen trees species had more axial parenchyma. Hence, this study revealed the specificity of xylem anatomy in karst tree species. Water and resource storage in xylem parenchyma are vital to karst trees (evergreens in particular) for their adaptation to the water-limiting environment.

**Key words** vessel; parenchyma; fibers; vessel wall reinforcement coefficient; theoretical hydraulic conductivity; trade-off

Ni MY, Antsara ANA, Wang YQ, Huang DL, Xiang W, Wan CY, Zhu SD (2021). Analysis of xylem anatomy and function of representative tree species in a mixed evergreen and deciduous broad-leaved forest of mid-subtropical karst region. *Chinese Journal of Plant Ecology*, 45, 394-403. DOI: 10.17521/cjpe.2020.0367

我国西南喀斯特是世界喀斯特连片分布面积最大的区域, 总面积超过55万km$^2$, 主要集中在广西、贵州和云南等省区(宋同清, 2015)。其中, 广西喀斯特分布面积达9.7万km$^2$, 喀斯特地貌富有特色(蒋忠诚等, 2007)。由于广西地处云贵高原的东南缘、南临北部湾, 受热带亚热带季风气候影响, 高温多雨, 岩溶作用强烈, 喀斯特地貌以峰丛洼地、峰丛谷地为主(袁道先, 1992)。与非喀斯特地区相比, 喀斯特环境具有岩石(碳酸盐岩)裸露程度高、土壤稀薄, 水分下渗快等特点(袁道先, 1992; 陈洪松等, 2013)。喀斯特生态系统较为脆弱, 受长期人类活动影响, 植被退化严重; 其中广西喀斯特石漠化面积达2.37万km$^2$, 生态环境问题突出(胡宝清, 2014)。广西喀斯特地区的植物多样性高(宋同清, 2015), 为喀斯特石漠化地区的植被重建提供了丰富的"乡土恢复工具树种库", 因此亟需了解喀斯特植物的生理生态适应性(曹坤芳等, 2014)。

由于喀斯特生境的水分有效性低, 喀斯特森林植物具有明显的旱生性特点(彭晚霞等, 2008)。喀斯特植物的生理生态适应性, 尤其是水分生理研究受到广泛关注(Wang *et al*., 2018; Chen *et al*., 2019)。研究表明喀斯特树种可以通过较强的生理调整能力适应水分亏缺(Cao *et al*., 2020), 或通过发达的根系扩大水分来源(Geekiyanage *et al*., 2019)。前期基于中亚热带喀斯特地区的喀斯特木本植物脆弱性曲线分析发现喀斯特树种抗栓塞能力并不高于同区域的非喀斯特森林树种(Fan *et al*., 2011; 谭凤森等, 2019)。另外, 研究发现植物薄壁细胞比例高的其非结构性碳水化合物含量高(Plavcová *et al*., 2016; Pratt & Jacobsen, 2017), 可能高的薄壁细胞比例在抗旱性方面发挥作用(Tomasella *et al*., 2019)。因此研究喀斯特树木的木质部结构特征有助于理解喀斯特植物的干旱适应性。

木本植物木质部主要由导管(或管胞)、纤维和薄壁细胞组成, 各自执行不同的功能: 导管(或管胞)负责水分和无机离子的运输; 薄壁组织负责水和碳水化合物的储存; 纤维主要负责机械支持(Hacke & Sperry, 2001; Plavcová & Jansen, 2015; Morris *et al*., 2016b)。木质部不同组织相互联系, 形成有机整体, 为植物体正常有序的生理过程提供保障(周朝彬等, 2016)。由于木质部空间(横截面积)限制, 导管组织、纤维组织、薄壁细胞组织的比例存在权衡关系, 即分配给某一组织较多的空间, 会减少其他组织的可用空间(Pratt & Jacobsen, 2017)。木质部组织分配的最优化有助于木质部发挥其最大的功能(Carlquist, 2018), 体现了其对生存环境的适应(Godfrey *et al*., 2020)。

广西木论喀斯特位于西南喀斯特的核心区域, 保存有连片面积最大、原生性较强的喀斯特森林(刘璐等, 2012)。顶极群落类型为中亚热带常绿落叶阔叶混交林; 与同区域的非喀斯特森林相比, 落叶树种的比例较高。落叶与常绿植物的生理生态特征具有显著差异; 基于木质部结构方面的研究表明落叶植物具有较低的木材密度、较小的导管密度以及较大的导管直径(Choat *et al*., 2005)。本研究选取木论喀斯特常绿落叶阔叶混交林21种典型树种(包括11种常绿树种和10种落叶树种), 测定枝条木质部解剖结构并计算相关水力功能性状。主要研究以下3个问题: (1)与全球数据相比, 喀斯特树种木质部解剖结构特征有何特殊性? (2)喀斯特树种木质部各组分之间是否具有显著的权衡关系? (3)喀斯特落叶与常绿树种的木质部结构和水力特征有何差异?

## 1 材料和方法

### 1.1 地理概况

研究样地位于广西河池市环江毛南族自治县木

 http://www.cjpe.ac.cn DOI: 10.17521/cjpe.2020.0367

植物生态学报 2021, 45 (4): 394–403
*Chinese Journal of Plant Ecology*

DOI: 10.17521/cjpe.2020.0367
http://www.plant-ecology.com

# 中亚热带喀斯特常绿落叶阔叶混交林典型树种的木质部解剖与功能特征分析

倪鸣源 ARITSARA Amy Ny Aina 王永强 黄冬柳 项 伟 万春燕 朱师丹*

广西大学亚热带农业生物资源保护与利用国家重点实验室, 南宁 530004, 广西大学林学院广西森林生态与保育重点实验室, 南宁 530004

**摘 要** 树木木质部主要由导管、纤维和薄壁组织组成, 分别具有运输、支撑和贮存的生理功能, 由于木质部空间限制, 一种组织比例的增加会导致其他组织比例的降低, 因而可能表现出权衡关系。分析木质部组织比例和权衡关系有助于了解植物的生理生态适应性。该研究选择中亚热带喀斯特常绿落叶阔叶混交林21种典型树种(10种落叶树种, 11种常绿树种), 测定枝条木质部各组织比例, 计算水力相关指标并分析性状之间的相关性。结果表明: (1)与全球木质部解剖数据对比分析, 喀斯特树种木质部趋向具有较高比例的薄壁组织; (2)喀斯特树种导管组织比例与薄壁和纤维组织比例之间没有显著的相关性, 但是薄壁和纤维组织比例之间有显著的权衡关系; (3)常绿和落叶树种的木质部水力运输安全性(导管壁加固系数)和效率性(理论导水率)均具有显著的权衡关系, 但是这两个类群线性回归的截距存在显著差异。即在相同的理论导水率条件下, 落叶树种比常绿树种具有较高的导管壁加固系数(安全性), 可能与常绿树种具有更多的轴向薄壁组织有关。喀斯特树种木质部解剖特征表明薄壁组织的贮存功能对喀斯特树种(尤其是常绿树种)的干旱适应具有重要作用。

**关键词** 导管组织; 薄壁组织; 纤维组织; 导管壁加固系数; 理论导水率; 权衡

倪鸣源, Aritsara ANA, 王永强, 黄冬柳, 项伟, 万春燕, 朱师丹 (2021). 中亚热带喀斯特常绿落叶阔叶混交林典型树种的木质部解剖与功能特征分析. 植物生态学报, 45, 394–403. DOI: 10.17521/cjpe.2020.0367

## Analysis of xylem anatomy and function of representative tree species in a mixed evergreen and deciduous broad-leaved forest of mid-subtropical karst region

NI Ming-Yuan, ARITSARA Amy Ny Aina, WANG Yong-Qiang, HUANG Dong-Liu, XIANG Wei, WAN Chun-Yan, and ZHU Shi-Dan*

*Guangxi Key Laboratory of Forest Ecology and Conservation, College of Forestry, Guangxi University, Nanning 530004, China; and State Key Laboratory for Conservation and Utilization of Subtropical Agro-bioresources, College of Forestry, Guangxi University, Nanning 530004, China*

**Abstract**

***Aims*** Vessel, fibers, and parenchyma are the main components of tree xylem. They are responsible for water transport, mechanical support, and water and nutrients storage. Given the limited xylem space, consistent investment in one type of tissue would constrain the space available for other types of tissue, thus resulting in a possible trade-off among different tissues in their fractions. Analysis of the fractions of tissue types in xylem and the trade-off would contribute to better understanding of the eco-physiological adaptation of plants.

***Methods*** We selected 21 characteristic tree species (10 deciduous and 11 evergreen) from a mixed evergreen and deciduous broad-leaved forest located in the mid-subtropical karst region, and measured their xylem tissue fractions. In addition, we calculated the hydraulic-related structural traits in xylems and examined the correlations among various traits.

***Important findings*** Compared to the global average values of xylem tissue fractions, the karst tree species tended to have a higher proportion of parenchyma. The fraction of vessel lumen was not correlated with fiber and parenchyma fractions across the tree species investigated. Instead, a significant trade-off was observed between fractions of fiber and parenchyma. A trade-off between the hydraulic efficiency (i.e. theoretical hydraulic conductivity) and safety (vessel wall reinforcement) was observed across both the deciduous and the evergreen tree species. The two contrasting group of karst trees differenced significantly in the intercepts of the lines for trade-offs. For

收稿日期Received: 2020-11-09 接受日期Accepted: 2021-01-18

基金项目: 广西八桂青年学者项目和广西自然科学基金(2017GXNSFBA198188)。Supported by the Guangxi Bagui Young Scholars Program and the Natural Science Foundation of Guangxi (2017GXNSFBA198188).

*通信作者Corresponding author (zhushidan@gxu.edu.cn)

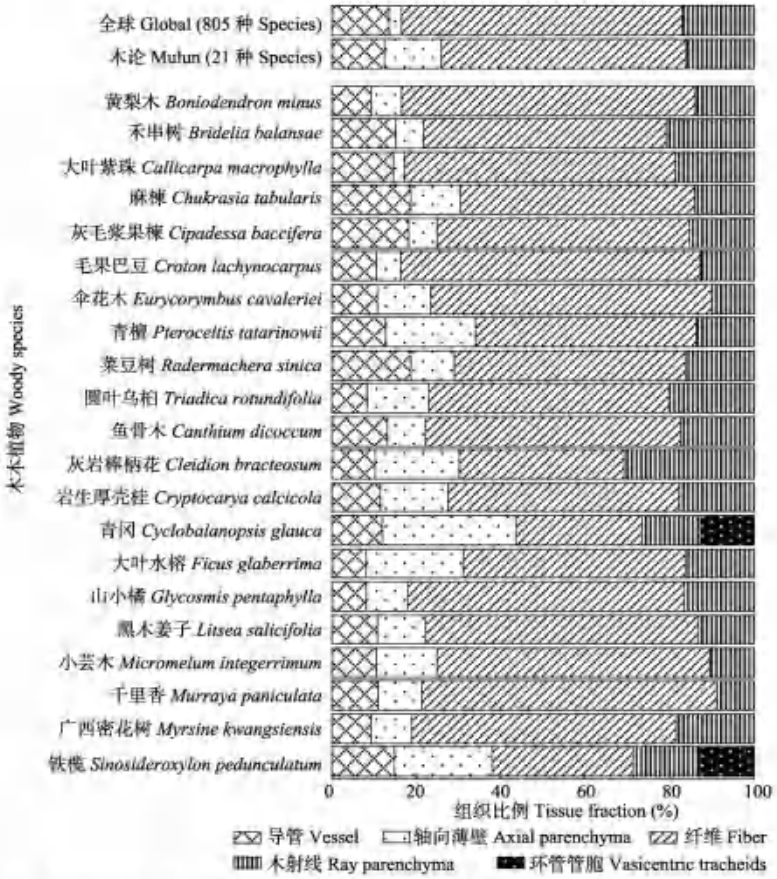


**图2** 基于TRY Database数据库的全球805种木本植物木质部各组分比例的平均值和广西木论21种喀斯特树种的木质部各组分的比例。

**Fig. 2** Xylem tissue partitioning of the 21 karst woody species in Mulun, Guangxi, and 805 woody species data downloaded from the TRY Database.

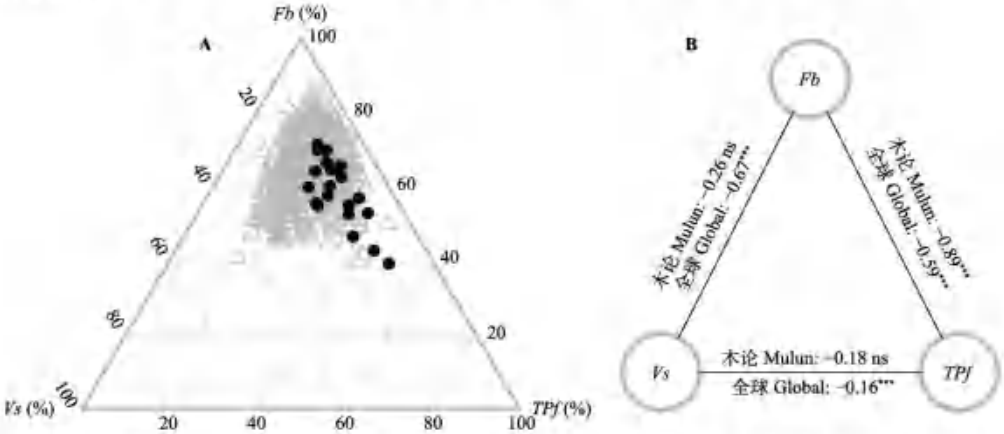


**图3** 喀斯特树种在全球木质部组织划分谱的位置(**A**)和木质部各组织比例之间的相关性(**B**)。●, 喀斯特树种; △, 全球数据(TRY)。*Fb*, 纤维组织比例; *TPf*, 薄壁组织比例; *Vs*, 导管组织比例。ns, $p > 0.05$, ***, $p < 0.001$。

**Fig. 3** Distributions of the karst woody species in the global xylem partitioning spectrum (**A**) and relationships among xylem tissue fractions (**B**). ●, karst woody species. △, global observations from TRY. *Fb*, fibers fraction; *TPf*, total parenchyma fraction; *Vs*, vessels fraction. ns, $p > 0.05$; ***, $p < 0.001$.

论国家级自然保护区的永久性监测样地(25.15° N, 108.04° E), 海拔420 m。受季风气候影响, 该样地年平均气温19.2 ℃, 年降水量1 529.2 mm, 雨季为4–8月, 降水量占全年的73.7% (刘璐等, 2012)。森林群落类型为中亚热带喀斯特常绿落叶阔叶混交林, 样地面积为1 $hm^2$ (100 m × 100 m), 东南向, 处于喀斯特峰丛洼地中上坡, 平均坡度约27°, 岩石裸露率80%–90% (郑颖吾, 1999)。样地共有物种44科73属95种; 重要值靠前的树种为青檀(*Pterocelti tatarinowii*)、广西密花树(*Myrsine kwangsiensis*)、千里香(*Murraya paniculata*)和菜豆树(*Radermachera sinica*)等。土壤以石灰土为主, 有机碳含量为15–24 g·$kg^{-1}$ (刘淑娟等, 2010; 宋同清, 2015)。

### 1.2 实验材料

取样时间为2019年8月, 选取样地中21种典型的喀斯特木本植物, 隶属于14科21属, 其中落叶10种, 常绿11种(表1)。根据树种的平均树高与胸径, 每种选取5株健康成熟个体, 从每个个体上剪取2段冠层阳生枝条, 长度5 cm, 直径为7–10 mm。

### 1.3 测定方法

将采回的新鲜枝条放入贴好标签的离心管中, 用FAA溶液固定一周后, 将样品固定在滑走切片机(Leica SM2010R, Leica, Nusslock, Germany)的凹槽进行横切, 切片厚度为25 μm, 用乙酸乙酯溶解泡沫(聚苯乙烯)的混合液涂抹样品切面防止切片变形(Barbosa *et al*., 2010), 用鸡蛋清和甘油的混合液把切片粘在载玻片上, 再用番红溶液和阿利新蓝溶液染色, 依次经过浓度为40%、70%、90%、100%的酒精脱水后用加拿大树胶固定。利用光学显微镜(Leica DM 3000, Leica, Wetzlar, Germany)观察并对木质部横切面(边材)进行拍照。每个个体制作2个切片, 每个切片分别在10、20、40倍镜下随机拍摄4个视野。

利用ImageJ 1.52软件(www.imagej.nih.gov, USA; Rueden *et al*., 2016)对染色后的切片图(图1)进行分析处理, 得出以下指标: (1)导管密度(*Vd*), 即单位视野内的导管数量(Perez-Harguindeguy *et al*., 2013), (2)导管比例(*Vs*)、环管管胞比例(*Tr*)、导管壁比例、轴向薄壁组织比例(*APf*)、射线组织比例(*RPf*)以及纤维组织比例(*Fb*), 其中薄壁组织在次生木质部中是由射线细胞和轴向薄壁细胞两部分活细胞组成(Morris *et al*., 2016a); (3)相连接两个导管的细胞壁厚度之和($t$)、相连接两个导管长短轴直径平均值($b$)(Hacke *et al*., 2001)。其中, 导管壁的加固系数为导管壁厚度($t$)与导管直径($b$)的比值。导管壁加固系数与枝条的栓塞脆弱性有很强的相关性, $t/b$越大, 抗栓塞能力越强(Hacke *et al*., 2001)。同时, 根据木质部导管结构特征, 计算以下水力相关性状:

**表1** 广西木论21种喀斯特树种的叶习性、胸径和树高(平均值±标准差)
**Table 1** Leaf types by longevity, diameter at breast height (*DBH*), and height of the 21 karst tree species studied in Muluo, Guangxi (mean ± *SD*)

| 物种 Species | 科 Family | 胸径 *DBH* (cm) | 树高 Height (m) |
|---|---|---|---|
| 落叶 Deciduous | | | |
| 黄梨木 *Boniodendron minus* | 无患子科 Sapindaceae | 12.4 ± 0.3 | 8.3 ± 0.2 |
| 禾串树 *Brideliu balansae* | 大戟科 Euphorbiaceae | 13.6 ± 1.0 | 7.5 ± 0.5 |
| 大叶紫珠 *Callicarpa macrophylla* | 马鞭草科 Verbenaceae | 6.5 ± 0.4 | 5.5 ± 0.7 |
| 麻楝 *Chukrasia tabularis* | 楝科 Meliaceae | 12.0 ± 1.4 | 8.0 ± 0.5 |
| 浆果楝 *Cipadessa baccifera* | 楝科 Meliaceae | 7.9 ± 1.1 | 6.4 ± 0.9 |
| 毛果巴豆 *Croton lachnocarpus* | 大戟科 Euphorbiaceae | 8.4 ± 0.3 | 6.5 ± 0.2 |
| 伞花木 *Eurycorymbus cavaleriei* | 无患子科 Sapindaceae | 10.6 ± 0.6 | 7.6 ± 0.3 |
| 青檀 *Pterocelti tatarinowii* | 榆科 Ulmaceae | 15.6 ± 0.6 | 8.7 ± 0.2 |
| 菜豆树 *Radermachera sinica* | 紫葳科 Bignoniaceae | 13.5 ± 0.5 | 8.3 ± 0.2 |
| 圆叶乌桕 *Triadica rotundifolia* | 大戟科 Euphorbiaceae | 15.8 ± 4.2 | 8.5 ± 0.3 |
| 常绿 Evergreen | | | |
| 假鱼骨木 *Psydrax dicoccu* | 茜草科 Rubiaceae | 9.2 ± 1.1 | 6.5 ± 0.5 |
| 灰岩棒柄花 *Cleidion bracteosum* | 大戟科 Euphorbiaceae | 7.3 ± 0.3 | 5.2 ± 0.2 |
| 岩生厚壳桂 *Cryptocarya calcicola* | 樟科 Lauraceae | 8.1 ± 0.4 | 6.5 ± 0.2 |
| 青冈 *Cyclobalanopsis glauca* | 壳斗科 Fagaceae | 10.9 ± 1.2 | 7.4 ± 0.6 |
| 大叶水榕 *Ficus glaberrima* | 桑科 Moraceae | 19.5 ± 3.4 | 7.7 ± 0.7 |
| 山小橘 *Glycosmis pentaphylla* | 芸香科 Rutaceae | 6.4 ± 0.3 | 4.3 ± 0.3 |
| 黑木姜子 *Litsea salicifolia* | 樟科 Lauraceae | 7.6 ± 0.8 | 6.8 ± 0.4 |
| 小芸木 *Micromelum integerrimum* | 芸香科 Rutaceae | 6.2 ± 1.1 | 5.3 ± 0.8 |
| 千里香 *Murraya paniculata* | 芸香科 Rutaceae | 6.4 ± 0.1 | 5.0 ± 0.2 |
| 广西密花树 *Myrsine kwangsiensis* | 紫金牛科 Myrsinaceae | 7.6 ± 0.3 | 6.1 ± 0.2 |
| 铁榄 *Sinosideroxylon pedunculatum* | 山榄科 Sapotaceae | 8.8 ± 0.4 | 6.5 ± 0.2 |

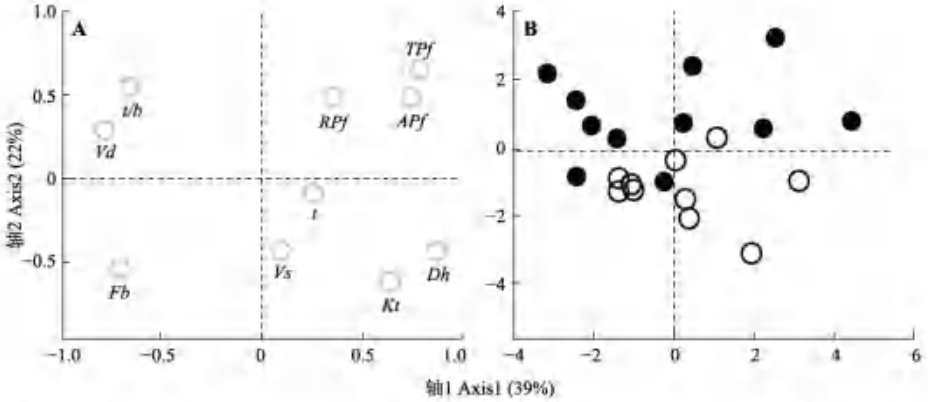


**图4** 广西木论喀斯特木本植物10个木质部性状(**A**)和21个树种(**B**)的主成分分析图。○, 落叶树种, ●, 常绿树种。*APf*, 轴向薄壁组织比例; *Dh*, 导管水力直径; *Fb*, 纤维组织比例; *Kt*, 理论导水率; *RPf*, 射线组织比例; *t*, 相连接两个导管的细胞壁厚度之和; *t/b*, 导管壁加固系数; *TPf*, 总的薄壁组织比例; *Vd*, 导管密度; *Vs*, 导管组织比例。

**Fig. 4** Principal component analysis for 10 xylem traits of woody plant (**A**), and 21 karst woody species (**B**) in Mulun, Guangxi. ○, deciduous; ●, evergreen. *APf*, axial parenchyma fraction; *Dh*, hydraulically-mean vessel diameter; *Fb*, fiber fraction; *Kt*, theoretical hydraulic conductivity; *RPf*, ray parenchyma fraction; *t*, double wall thickness measured from vessel pairs; *t/b*, vessel wall reinforcement coefficient; *TPf*, total parenchyma fraction; *Vd*, vessel density; *Vs*, vessel lumen fraction.

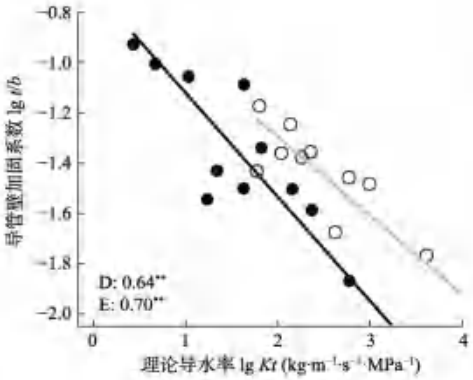


**图5** 广西木论喀斯特21个树种导管壁加固系数(*t/b*)与理论导水率(*Kt*)的相关关系的简化主轴回归分析。○: 落叶树种(D), ●: 常绿树种(E)。落叶树种回归方程(灰色): $y = -0.31x - 0.67$; 常绿树种回归方程(黑色): $y = -0.41x - 0.71$。**, $p < 0.01$。

**Fig. 5** Reduced major axis regression of vessel wall reinforcement coefficient (*t/b*) and theoretical hydraulic conductivity (*Kt*) of 21 karst woody species in Mulun, Guangxi. ○, deciduous (D), ●, evergreen (E). Linear regression of deciduous species (grey): $y = -0.31x - 0.67$; linear regression of evergreen species (black): $y = -0.41x - 0.71$ **, $p < 0.01$.

## 3 讨论

### 3.1 喀斯特树种木质部具有较小的导管水力直径和较大比例的轴向薄壁组织

与全球木本植物木质部解剖结构数据相比, 喀斯特树木的木质部趋于具有较高比例的轴向薄壁组织(图2)。已有研究表明薄壁组织具有贮存水分、储存和转运碳水化合物的功能(Plavcova & Jansen, 2015; Morris *et al*., 2016b), 在维持植物水分平衡(Meinzer *et al*., 2009)和修复导管栓塞过程中发挥重要作用(Zwieniecki & Holbrook, 2009; Tomasella *et al*., 2019)。木质部中高的薄壁组织比例具有高的水容(Secchi *et al*., 2017; Santiago *et al*., 2018), 当土壤有效水分供给不足时, 高的水容可以缓解土壤与叶片的水势差, 从而维持叶片的气体交换(McCulloh *et al*., 2019; Siddiq *et al*., 2019)。最近对温带石灰岩山地的19种阔叶树种的研究发现, 木质部薄壁细胞比例与抗栓塞能力具有显著的负相关关系(Chen *et al*., 2020)。以上研究结果证明了薄壁细胞的贮存能力对喀斯特树种的干旱适应具有重要作用(谭凤森等, 2019), 也解释了中亚热带喀斯特树种较低的抗栓塞能力(Fan *et al*., 2011)。

本研究中喀斯特21种树种木质部导管水力直径(平均值为44.76 μm)显著地低于全球木本植物的平均值(94.43 μm; Morris *et al*., 2018)。在西南热带喀斯特森林的研究也发现喀斯特树种的导管直径要显著地低于临近的沟谷雨林树种(Zhu *et al*., 2017), 体现了对喀斯特旱生生境的水力适应(Hacke *et al*., 2017)。与其他树种不同, 青冈和铁榄的木质部导管周围具有直径较小的环管管胞(图2), 而且它们主要分布在喀斯特峰丛洼地上坡更为干旱的生境。同样,

 http://www.cjcn.org.cn DOI: 10.17521/cjpe.2020.0367

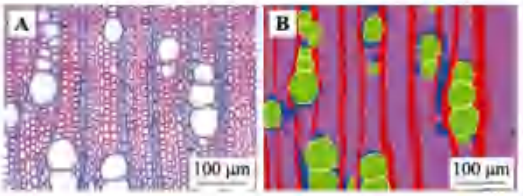


**图1** 菜豆树木质部染色切片(**A**)和经过人工辨别和绘制后的木质部组织结构分布图(**B**)。绿色，导管管腔；黄色，导管壁；红色，射线细胞，蓝色，轴向薄壁细胞，紫色，纤维细胞。

**Fig. 1** A stained xylem cross-section image of *Radermachera sinica* (**A**), and the same image in which different xylem tissues were manually coded with different colors (**B**). Green, vessel lumen; Yellow, vessel wall; Red, ray parenchyma; Blue, axial parenchyma; Purple, fibers.

(1)导管水力直径(*Dh*)的计算公式参照Tyree和Zimmermann (2002):

$$Dh = \sqrt[4]{\frac{\sum_{i=1}^{n} b_i^4}{n}} \quad (1)$$

式中，$b_i$表示单个导管长短轴直径的平均值。

(2)理论导水率(*Kt*)，反映木质部水分运输的效率性。计算公式参照Tyree和Zimmermann (2002):

$$Kt = \frac{\rho\pi}{128\eta} \times Vd \times Dh^4 \quad (2)$$

式中，*Vd*表示导管密度，*Dh*表示导管水力直径，$\rho$表示20 ℃下水的密度998.2 kg·m$^{-3}$；$\eta$表示20 ℃下水的黏度1.002 × 10$^{-9}$ MPa·s。

### 1.4 数据分析

全球木本植物木质部组织比例数据从TRY Database (Kattge *et al*., 2020)下载，利用R 3.5.0软件进行统计分析。用ggtern软件(Hamilton & Ferry, 2018)绘制木论和全球的木质部组织比例三角坐标图；用stats R软件中的t.test公式分析常绿与落叶树种木质部解剖结构和水力特征的差异显著性；用factoextra软件的PCA公式做主成分分析。利用smatr R软件中的sma公式通过简化主轴回归分析(Warton *et al*., 2012)来分析木论和全球树种木质部各组织比例之间的相关性、理论导水率与导管壁加固系数的相关性，以及落叶与常绿树种直线回归斜率和截距的差异性。所有图用R-package软件的base绘制。

## 2 结果

### 2.1 喀斯特树种木质部解剖特征与全球木本植物数据的比较

本研究测定的喀斯特树种木质部轴向薄壁组织比例的种间变异较大(变异系数为54.6%)，最低值为2.6% (大叶紫珠(*Callicarpa macrophylla*))，最高值为31.0% (青冈(*Cyclobalanopsis glauca*))。射线组织比例的变异系数是29.1%，最小值是8.7% (千里香)，最大值是29.6% (灰岩棒柄花(*Cleidion bracteosum*))。导管组织比例的种间差异相对较小，变异系数为26.2% (图2，附录I)。铁榄(*Sinosideroxylon pedunculatum*)和青冈的导管周围有环管管胞，其环管管胞面积分别占木质部横截面积的12.1%和12.6% (图2，附录II)。与全球木本植物木质部组织比例数据对比分析，本研究21种喀斯特树种木质部纤维组织和导管组织比例分别为全球数据平均值的87%和90% (图2)，但是这些喀斯特树种的木质部趋于具有较高比例的轴向薄壁组织，其平均值是全球数据平均值的4.3倍(图2，图3A)。

### 2.2 喀斯特树种木质部各组分之间的权衡关系

基于全球805种木本植物木质部解剖结构数据，各组分比例之间存在显著的权衡关系。喀斯特树种木质部各组织比例的相关关系与全球数据的分析结果不完全一致：喀斯特树种的纤维组织比例与薄壁组织比例存在显著的权衡关系，但是导管组织比例与纤维组织比例和薄壁组织比例均不存在显著的相关关系(图3B)。

### 2.3 喀斯特常绿与落叶树种木质部水力特征的差异

主成分分析结果表明第1轴解释总变异的39%，与木质部导管的管径(*Dh*、*Vd*)相关；第2轴解释总变异的22%，与木质部的贮存(*TPf*)和水分传导率(*Kt*)相关(图4A)。常绿和落叶树种在第2轴可以显著区分为两个类群，常绿树种具有较多的轴向薄壁细胞和较低的理论导水率($p < 0.001$；图4B；附录I)。不论常绿树种还是落叶树种，理论导水率和导管壁加固系数之间均呈显著的负相关关系；但是这两个植物类群的直线回归方程的截距具有显著差异($p = 0.002$)，即在理论导水率相同情况下，落叶树种具有更高的导管壁加固系数(图5)。

 http://DOI:10.17521/cjpe.2020.0367

variation and its storage function of ray tissue. *Journal of Northwest Forestry University*, 31, 179-183. [周朝彬, 胡霞, 宋于洋, 龚伟, 胡庭兴 (2016). 射线组织径向变异及其贮藏功能研究进展. 西北林学院学报, 31, 179-183.]

Zhu SD, Chen YJ, Fu PL, Cao KF (2017). Different hydraulic traits of woody plants from tropical forests with contrasting soil water availability. *Tree Physiology*, 37, 1469-1477.

Zwieniecki MA, Holbrook NM (2009). Confronting Maxwell's demon: biophysics of xylem embolism repair. *Trends in Plant Science*, 14, 530-534.

特邀编委: 黄建国　责任编辑: 李　敏

**附录 I　21 个喀斯特树种的木质部特征(平均值±标准差)**

**Supplement I　Xylem characteristics of the 21 karst woody species from Mulun, Guangxi (mean ± *SD*)**

https://www.plant-ecology.com/fileup/1005-264X/PDF/cjpe.2020.0367-S1.pdf

**附录 II　广西木论 21 种喀斯特树种的木质部染色切片图**

**Supplement II　Xylem anatomical structure the 21 karst woody species in Mulun, Guangxi**

https://www.plant-ecology.com/fileup/1005-264X/PDF/cjpe.2020.0367-S2.pdf



DOI: 10.17521/cjpe.2020.0367

在加利福尼亚南部干旱灌木林(Hacke, 2015)和海南红树林(邓传远等, 2015)也发现优势树种木质部存在环管管胞。环管管胞本身除了具有水分运输的功能外，当植物面临水分胁迫时还能够连接被栓塞阻隔的导管，从而保证了水分运输的安全性(Carlquist, 2001)。喀斯特树种的环管管胞的生理作用值得进一步探讨。

### 3.2 喀斯特树种木质部各组分间的权衡关系

与全球数据的分析结果不同，喀斯特树种木质部导管组织比例与其他组织比例之间的相关性均不显著(图3)。这一结果与加利福尼亚干旱森林树种的研究结果(Pratt & Jacobsen, 2017)相似，可能与这些木本植物具有相对稳定的导管组织比例有关。喀斯特树种木质部纤维组织比例与薄壁组织比例存在显著的权衡关系(图3)，这些树种的木质部倾向于具有较高的薄壁组织比例而不是纤维组织，它们可能通过提高栓塞修复能力(而非抗栓塞能力)适应干旱(Pratt & Jacobsen, 2017; Janssen *et al*., 2020; Aritsara *et al*., 2021)。较低的纤维组织比例(支撑作用)也从木质部结构的角度解释了为什么中亚热带的喀斯特森林冠层高度要显著低于同区域的亚热带常绿阔叶林(平均林冠高度为28.90 m; Liu *et al*., 2019)。

### 3.3 喀斯特落叶与常绿树种木质部解剖和水力特征的差异

本研究发现喀斯特落叶与常绿树种的导管水力直径和导管密度没有显著差异，但是落叶树种的理论导水率是常绿树种的两倍(附录I)。根据Hagen-Poiseuille定理，理论导水率与导管直径的4次方成正比，导管直径的较小差异(喀斯特落叶树种比常绿树种的平均值高25%)，导致理论导水率的较大变化。本研究发现木质部水分运输效率性(理论导水率)与安全性(导管壁加固系数)之间存在权衡关系，但是落叶与常绿树种具有显著差异：若导管壁加固系数相同，落叶树种具有较高的水分运输效率；如导水率相同，常绿树种反而具有较低的抗栓塞能力。这与以往研究发现同一森林中常绿植物比落叶植物具有更强的抗栓塞能力的结果相反(Chen *et al*., 2009; Fu *et al*., 2012)，原因可能在于本研究的喀斯特常绿树种具有丰富的轴向薄壁细胞(附录I)，并不依赖强的抗栓塞能力适应干旱。

通过长期的隔离降雨模拟试验，结果发现干旱加剧会导致热带季节性森林中落叶植物成分显著增加(Aguirre-Gutierrez *et al*., 2019)。在气候变化背景下，我国亚热带地区呈现显著的干热化趋势(Qu & Huang, 2018; Yin *et al*., 2018)。由于亚热带喀斯特森林对气候变化的响应较为敏感，干旱程度的增加将会影响喀斯特森林群落的组成和物种多样性，并进一步影响森林生态系统的结构和功能。基于喀斯特树种木质部解剖结构和水力特征的研究有助于了解它们对干旱的水力适应，从而提高对树种动态变化的预测性。

## 4 结论

本研究揭示了中亚热带喀斯特森林树种木质部普遍具有较高比例的薄壁组织，表明薄壁组织的贮存和修复能力对维持喀斯特树种木质部的水力安全至关重要。对喀斯特常绿和落叶树种木质部特征的比较结果表明，落叶树种木质部倾向于提高水分运输效率，而常绿树种则倾向于投资更多的薄壁组织用于调节水分平衡。结合喀斯特树种木质部功能性状与树种动态变化(生长和死亡)的研究有助于理解喀斯特森林对气候变化的响应。

**致谢** 感谢广西大学林学院的宋慧清、曾文豪和张启伟同学在野外采样和实验测定工作中给予的帮助。

## 参考文献

Aguirre-Gutierrez J, Oliveras I, Rifai S, Fauset S, Adu-Bredu S, Affum-Baffoe K, Baker TR, Feldpausch TR, Gvozdevaite A, Hubau W, Kraft NJB, Lewis SL, Moore S, Niinemets Ü, Peprah T, Phillips OL, Ziemińska K, Enquist B, Malhi Y (2019). Drier tropical forests are susceptible to functional changes in response to a long-term drought. *Ecology Letters*, 22, 855-865.

Aritsara ANA, Razakandraibe VM, Ramananantoandro T, Gleason SM, Cao KF (2021). Increasing axial parenchyma fraction in the Malagasy Magnoliids facilitated the co-optimization of hydraulic efficiency and safety. *New Phytologist*, 229, 1467-1480.

Barbosa ACF, Pace MR, Witovisk L, Angyalossy V (2010). A new method to obtain good anatomical slides of heterogeneous plant parts. *IAWA Journal*, 31, 373-383.

Cao KF, Fu PL, Chen YJ, Jiang YJ, Zhu SD (2014). Implications of the ecophysiological adaptation of plants on tropical karst habitats for the ecological restoration of desertified rocky lands in Southern China. *Scientia Sinica Vitae*, 44, 238-247. [曹坤芳, 付培立, 陈亚军, 姜艳娟, 朱师丹 (2014). 热带岩溶植物生理生态适应性对于南方石漠化

土地生态重建的启示. 中国科学: 生命科学, 44, 238-247.]

Cao M, Wu C, Liu JC, Jiang YJ (2020). Increasing leaf $\delta^{13}C$ values of woody plants in response to water stress induced by tunnel excavation in a karst trough valley: implication for improving water-use efficiency. *Journal of Hydrology*, 586, 124895. DOI: 10.1016/j.jhydrol.2020.124895.

Carlquist S (2018). Living cells in wood 3. Overview: Functional anatomy of the parenchyma network. *Botanical Review*, 84, 242-294.

Carlquist SJ (2001). *Comparative Wood Anatomy*. Springer, Berlin. 448.

Chen HS, Nie YP, Wang KL (2013). Spatio-temporal heterogeneity of water and plant adaptation mechanisms in karst regions: a review. *Acta Ecologica Sinica*, 33, 317-326. [陈洪松, 聂云鹏, 王克林 (2013). 岩溶山区水分时空异质性及植物适应机理研究进展. 生态学报, 33, 317-326.]

Chen ZC, Li S, Luan JW, Zhang YT, Zhu SD, Wan XC, Liu SR (2019). Prediction of temperate broadleaf tree species mortality in arid limestone habitats with stomatal safety margins. *Tree Physiology*, 39, 1428-1437.

Chen ZC, Zhu SD, Zhang YT, Luan JW, Li S, Sun PS, Wan XC, Liu SR (2020). Tradeoff between storage capacity and embolism resistance in the xylem of temperate broadleaf tree species. *Tree Physiology*, 40, 1029-1042.

Choat B, Ball MC, Luly JG, Holtum JAM (2005). Hydraulic architecture of deciduous and evergreen dry rainforest tree species from north-eastern Australia. *Trees*, 19, 305-311.

Deng CY, Zheng JM, Zhang WC, Guo SZ, Xue QH, Ye LY, Sun JW (2015). Ecological wood anatomy of *Rhizophora stylosa*. *Chinese Journal of Plant Ecology*, 39, 604-615. [邓传远, 郑俊鸣, 张万超, 郭素枝, 薛秋华, 叶露莹, 孙建文 (2015). 红海榄木材结构的生态解剖. 植物生态学报, 39, 604-615.]

Fan DY, Jie SL, Liu CC, Zhang XY, Xu XW, Zhang SR, Xie ZQ (2011). The trade-off between safety and efficiency in hydraulic architecture in 31 woody species in a karst area. *Tree Physiology*, 31, 865-877.

Fu PL, Jiang YJ, Wang AY, Brodribb TJ, Zhang JL, Zhu SD, Cao KF (2012). Stem hydraulic traits and leaf water-stress tolerance are co-ordinated with the leaf phenology of angiosperm trees in an Asian tropical dry karst forest. *Annals of Botany*, 110, 189-199.

Geekiyanage N, Goodale UM, Cao KF, Kitajima K (2019). Plant ecology of tropical and subtropical karst ecosystems. *Biotropica*, 51, 626-640.

Godfrey JM, Riggio J, Orozco J, Guzmán-Delgado P, Chin ARO, Zwieniecki MA (2020). Ray fractions and carbohydrate dynamics of tree species along a 2750 m elevation gradient indicate climate response, not spatial storage limitation. *New Phytologist*, 225, 2314-2330.

Hacke UG (2015). *Functional and Ecological Xylem Anatomy*. Springer International Publishing, Cham, Switzerland.

Hacke UG, Sperry JS (2001). Functional and ecological xylem anatomy. *Perspectives in Plant Ecology, Evolution and Systematics*, 4, 97-115.

Hacke UG, Sperry JS, Pockman WT, Davis SD, McCulloh KA (2001). Trends in wood density and structure are linked to prevention of xylem implosion by negative pressure. *Oecologia*, 126, 457-461.

Hacke UG, Spicer R, Schreiber SG, Plavcová L (2017). An ecophysiological and developmental perspective on variation in vessel diameter. *Plant, Cell & Environment*, 40, 831-845.

Hamilton NE, Ferry M (2018). Ggtern: Ternary Diagrams Using ggplot2. *Journal of Statistical Software*, 87, 1-17.

Hu BQ (2014). *Study on Human-Land Systems in Karst Areas*. Science Press, Beijing. 596. [胡宝清 (2014). 喀斯特人地系统研究. 科学出版社, 北京. 596.]

Janssen TAJ, Hölttä T, Fleischer K, Naudts K, Dolman H (2020). Wood allocation trade-offs between fiber wall, fiber lumen, and axial parenchyma drive drought resistance in neotropical trees. *Plant, Cell & Environment*, 43, 965-980.

Jiang ZC, Li XK, Zeng FP (2007). *Ecological Reconstruction in Peak Cluster Karst Depression*. Geological Publishing House, Beijing. 151. [蒋忠诚, 李先琨, 曾馥平 (2007). 岩溶峰丛洼地生态重建. 地质出版社, 北京. 151.]

Kattge J, Bönisch G, Díaz S, Lavorel S, Prentice I, Leadley P (2020). TRY plant trait database—Enhanced coverage and open access. *Global Change Biology*, 26, 119-188.

Liu H, Gleason SM, Hao GY, Hua L, He PC, Goldstein G, Ye Q (2019). Hydraulic traits are coordinated with maximum plant height at the global scale. *Science Advances*, 5, eaav1332. DOI: 10.1126/sciadv.aav1332.

Liu L, Song TQ, Peng WX, Wang KL, Du H, Lu SY, Zeng FP (2012). Spatial heterogeneity of soil microbial biomass in Mulun National Nature Reserve in karst area. *Acta Ecologica Sinica*, 32, 207-214. [刘璐, 宋同清, 彭晚霞, 王克林, 杜虎, 鲁士杨, 曾馥平 (2012). 木论喀斯特自然保护区土壤微生物生物量的空间格局. 生态学报, 32, 207-214.]

Liu SJ, Zhang W, Wang KL, Chen HS, Wei GF (2010). Spatio-temporal heterogeneity and its formation causes of soil physical properties in karst peak-cluster depression area of northwest Guangxi, China. *Chinese Journal of Applied Ecology*, 21, 2249-2256. [刘淑娟, 张伟, 王克林, 陈洪松, 韦国富 (2010). 桂西北喀斯特峰丛洼地土壤物理性质的时空分异及成因. 应用生态学报, 21, 2249-2256.]

McCulloh KA, Domec JC, Johnson DM, Smith DD, Meinzer FC (2019). A dynamic yet vulnerable pipeline: integration and coordination of hydraulic traits across whole plants. *Plant, Cell & Environment*, 42, 2789-2807.

Meinzer FC, Johnson DM, Lachenbruch B, McCulloh KA, Woodruff DR (2009). Xylem hydraulic safety margins in

 http://www.cjpe.ac.cn DOI: 10.17521/cjpe.2020.0367

woody plants: coordination of stomatal control of xylem tension with hydraulic capacitance. *Functional Ecology*, 23, 922-930.

Morris H, Gillingham MAF, Plavcová L, Gleason SM, Olson ME, Coomes DA, Fichtler E, Klepsch MM, Martinez-Cabrera HI, McGlinn DJ, Wheeler EA, Zheng JM, Ziemińska K, Jansen S (2018). Vessel diameter is related to amount and spatial arrangement of axial parenchyma in woody angiosperms. *Plant, Cell & Environment*, 41, 245-260.

Morris H, Brodersen C, Schwarze FWMR, Jansen S (2016a). The parenchyma of secondary xylem and its critical role in tree defense against fungal decay in relation to the CODIT model. *Frontiers in Plant Science*, 7, 1665. DOI: 10.3389/fpls.2016.01665.

Morris H, Plavcová L, Cvecko P, Fichtler E, Gillingham MAF, Martinez-Cabrera HI, McGlinn DJ, Wheeler E, Zheng JM, Ziemińska K, Jansen S (2016b). A global analysis of parenchyma tissue fractions in secondary xylem of seed plants. *New Phytologist*, 209, 1553-1565.

Peng WX, Wang KL, Song TQ, Zeng FP, Wang JR (2008). Controlling and restoration models of complex degradation of vulnerable karst ecosystem. *Acta Ecologica Sinica*, 28, 811-820. [彭晚霞, 王克林, 宋同清, 曾馥平, 王久荣 (2008). 喀斯特脆弱生态系统复合退化控制与重建模式. 生态学报, 28, 811-820.]

Pérez-Harguindeguy N, Díaz S, Garnier E, Lavorel S, Poorter H, Jaureguiberry P, Bret-Harte MS, Cornwell WK, Craine JM, Gurvich DE, Urcelay C, Veneklaas EJ, Reich PB, Poorter L, Wright IJ, *et al* (2013). New handbook for standardised measurement of plant functional traits worldwide. *Australian Journal of Botany*, 61, 167. DOI: 10.1071/bt12225.

Plavcová L, Hoch G, Morris H, Ghiasi S, Jansen S (2016). The amount of parenchyma and living fibers affects storage of nonstructural carbohydrates in young stems and roots of temperate trees. *American Journal of Botany*, 103, 603-612.

Plavcova L, Jansen S (2015). The role of xylem parenchyma in the storage and utilization of nonstructural carbohydrates// Hacke U. *Functional and Ecological Xylem Anatomy*. Springer International Publishing, Cham, Switzerland: 209-234.

Pratt RB, Jacobsen AL (2017). Conflicting demands on angiosperm xylem: tradeoffs among storage, transport and biomechanics. *Plant, Cell & Environment*, 40, 897-913.

Qu X, Huang G (2018). Different multi-year mean temperature in mid-summer of South China under different 1.5 °C warming scenarios. *Scientific Reports*, 8, 13794. DOI: 10.1038/s41598-018-32277-6.

Rueden CT, Hiner MC, Eliceiri KW (2016). ImageJ: image analysis interoperability for the next generation of biological image data. *Microscopy and Microanalysis*, 22, 2066-2067.

Santiago LS, de Guzman ME, Baraloto C, Vogenberg JE, Brodie M, Hérault B, Fortunel C, Bonal D (2018). Coordination and trade-offs among hydraulic safety, efficiency and drought avoidance traits in Amazonian rainforest canopy tree species. *New Phytologist*, 218, 1015-1024.

Secchi F, Pagliarani C, Zwieniecki MA (2017). The functional role of xylem parenchyma cells and aquaporins during recovery from severe water stress. *Plant, Cell & Environment*, 40, 858-871.

Siddiq Z, Zhang YJ, Zhu SD, Cao KF (2019). Canopy water status and photosynthesis of tropical trees are associated with trunk sapwood hydraulic properties. *Plant Physiology and Biochemistry*, 139, 724-730.

Song TQ (2015). *Plants and Environment in Karst Areas of Southwest China*. Science Press, Beijing: 607. [宋同清 (2015). 西南喀斯特植物与环境. 科学出版社, 北京: 607.]

Tan FS, Song HQ, Li ZG, Zhang QW, Zhu SD (2019). Hydraulic safety margin of 17 co-occurring woody plants in a seasonal rain forest in Guangxi's Southwest karst landscape, China. *Chinese Journal of Plant Ecology*, 43, 227-237. [谭凤森, 宋慧洁, 李忠国, 张启伟, 朱师丹 (2019). 桂西南喀斯特季雨林木本植物的水力安全. 植物生态学报, 43, 227-237.]

Tomasella M, Petrussa E, Petruzzellis F, Nardini A, Casolo V (2019). The possible role of non-structural carbohydrates in the regulation of tree hydraulics. *International Journal of Molecular Sciences*, 21: E144. DOI: 10.3390/ijms21010144.

Tyree MT, Zimmermann MH (2002). *Xylem Structure and the Ascent of Sap*. 2nd ed. Springer Heidelberg, Berlin.

Wang J, Wen XF, Zhang XY, Li SG (2018). The strategies of water-carbon regulation of plants in a subtropical primary forest on karst soils in China. *Biogeosciences*, 15, 4193-4203.

Warton DI, Duursma RA, Falster DS, Taskinen S (2012). Smatr 3—An R package for estimation and inference about allometric lines. *Methods in Ecology and Evolution*, 3, 257-259.

Yin YH, Ma DY, Wu SH (2018). Climate change risk to forests in China associated with warming. *Scientific Reports*, 8, 493. DOI: 10.1038/s41598-017-18798-6.

Yuan DX (1992). Karst in southwest China and its comparison with karst in North China. *Quaternary Sciences*, 12, 352-361. [袁道先 (1992). 中国西南部的岩溶及其与华北岩溶的对比. 第四纪研究, 12, 352-361.]

Zheng YW (1999). *Introduction to Mulun Karst Forest Region*. Science Press, Beijing: 254. [郑绵普 (1999). 木论喀斯特林区概论. 科学出版社, 北京: 254.]

Zhou CB, Hu X, Song YY, Gong W, Hu TX (2016). Radial

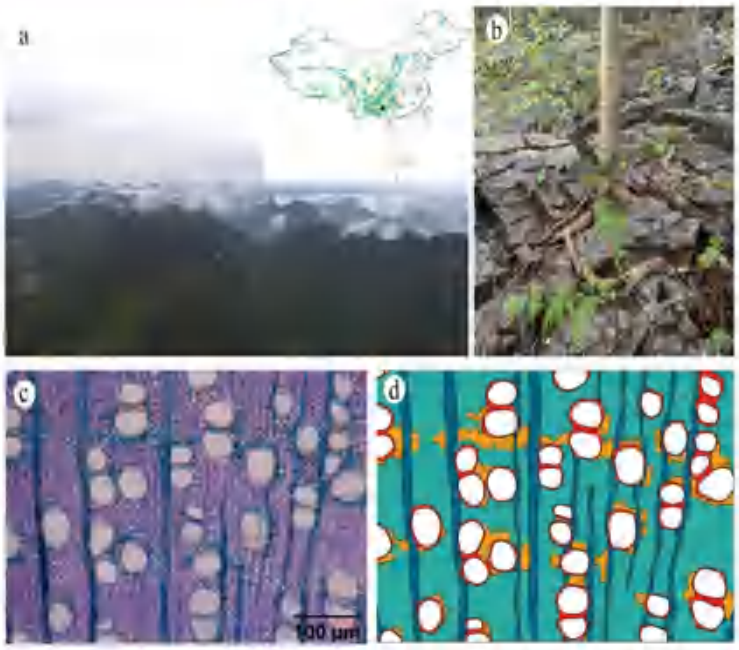


Figure 1. (a) Location and scenery view of the karst habitat within the study site. Karst formation distribution (green) in China is shown on the inset map. (b) Karst tree growing on a rocky substrate. (c) Xylem transversal section of *B. minus* to illustrate tissue fraction and (d) tissue fraction and arrangement analysis with the same scaling as panel (c). Vessel lumina are shown in white, vessel walls are in red, rays are in blue, axial parenchyma are in orange and fibers are in cyan.

(Rennolls 1978, Vallet and Perot 2016). Furthermore, 95% of the trees have a *DBH* of <25 cm. *Pteroceltis tatarinowii*, *Radermachera sinica* and *Chukrasia tabularis* are the most dominant species. The mean annual rainfall is 1529 mm, 73.7% of which falls between April and August. Further, the mean monthly temperature varies from 9.3 °C in January to 26.9 °C in July, with an annual average of 19.3 °C (China Meteorological Data Service Center, https://data.cma.cn/en).

We selected 21 co-occurring woody plant species from a 1-ha permanent plot (Table 1) and one particularly abundant species in the region's karst habitats (Lu et al. 2021). The importance value index (IVI) of each species was calculated by summing its relative frequency, density and basal area (Cottam and Curtis 1956), and the studied species were selected homogeneously along the IVI range. The 22 selected species differed in leaf habits; namely, 15 species are evergreen and seven are deciduous.

### Growth rate and dynamics

An improvised apparatus made of stainless belts tightened with a spring was installed at 1.30 m height on 3–185 random trees per species (all with *DBH* greater than 5 cm) in July 2018 to measure tree growth increment. Growth increment was monitored annually for 3 years (2019, 2020 and 2021). The growth rate was quantified as the yearly average of *DBH* increase across the 3 years as follows:

$$DGR_i = \frac{\sum_{t=0}^{n}(DBH_{t+1} - DBH_t)}{n} \quad (1)$$

With the observation of different growth rates of large and small trees during growth monitoring campaigns, size–growth scaling relationships were analyzed following Iida et al. (2014):

$$R_i = r_{1j} + r_{2j} \cdot \ln(D_{1i}) \quad (2)$$

$$\ln(D_{2i}) = \ln(D_{1i}) + R_i \cdot (t_{1i} - t_{2i}) \quad (3)$$

where $R_i$ is the relative growth rate of each species, and $r_{1j}$ and $r_{2j}$ are the model's intercept and slope, respectively. Thus, a positive $r_{2j}$ suggests an increase in growth rate with increasing *DBH* thus, $r_{2j}$ quantifies "growth acceleration." $D_{1i}$ and $D_{2i}$ are the diameters of the tree $i$ in consecutive years 1 ($t_{1i}$) and 2 ($t_{2i}$), respectively. The correlations between hydraulic traits and $r_{2j}$ were analyzed only across species for which Eq. (2) was significant.

### Hydraulic conductivity and embolism resistance

Samples from individuals growing near the inventory plot were collected in the early morning. For each of the 22 species, branches were collected from at least five individuals, except for

Tree Physiology 00, 1–12
https://doi.org/10.1093/treephys/tpad050

Research paper

# Tree growth is correlated with hydraulic efficiency and safety across 22 tree species in a subtropical karst forest

Amy N. A. Aritsara[1,2,†], Ming-Yuan Ni[3,†], Yong-Qiang Wang[1], Chao-Long Yan[1], Wen-Hao Zeng[1], Hui-Qing Song[1], Kun-Fang Cao[1] and Shi-Dan Zhu[1,4]

[1]State Key Laboratory for Conservation and Utilization of Subtropical Agro-Bioresources, Guangxi Key Laboratory of Forest Ecology and Conservation, College of Forestry, Guangxi University, No. 100 Daxuedonglu Road, Nanning 530004, Guangxi, China; [2]College of Life Sciences and Technology, Guangxi University, No. 100 Daxuedonglu Road, Nanning 530004, Guangxi, China; [3]School of Basic Medical Sciences, Youjiang Medical University for Nationalities, No. 98 Chengxiang Road, Baise 533000, Guangxi, China; [4]Corresponding author (zhushidan@gxu.edu.cn)

Received August 25, 2022; accepted April 12, 2023; handling Editor Maurizio Mencuccini

**Karst forests are habitats in which access to soil water can be challenging for plants. Therefore, safe and efficient xylem water transport and large internal water storage may benefit tree growth. In this study, we selected 22 tree species from a primary subtropical karst forest in southern China and measured their xylem anatomical traits, saturated water content (SWC), hydraulic conductivity ($K_s$) and embolism resistance ($P_{50}$). Additionally, we monitored growth of diameter at breast height (DBH) in 440 individual trees of various sizes over three consecutive years. Our objective was to analyze the relationships between xylem structure, hydraulic efficiency, safety, water storage and growth of karst tree species. The results showed significant differences in structure but not in hydraulic traits between deciduous and evergreen species. Larger vessel diameter, paratracheal parenchyma and higher *SWC* were correlated with higher $K_s$. Embolism resistance was not correlated with the studied anatomical traits, and no tradeoff with $K_s$ was observed. In small trees (5–15 cm *DBH*), diameter growth rate (DGR) was independent of hydraulic traits. In large trees (>15 cm *DBH*), higher $K_s$ and more negative $P_{50}$ accounted for higher DGR. From lower to greater embolism resistance, the size–growth relationship shifted from growth deceleration to acceleration with increasing tree size in eight of the 22 species. Our study highlights the vital contributions of xylem hydraulic efficiency and safety to growth rate and dynamics in karst tree species; therefore, we strongly recommend their integration into trait-based forest dynamic models.**

*Keywords*: embolism resistance, hydraulic efficiency, karst forest, tree growth, water storage, xylem anatomy, xylem parenchyma.

## Introduction

Carbon and water cycles are strongly associated with evapotranspiration and primary production in plants. The rate of water transpiration from leaves is strongly and positively correlated with the leaf photosynthetic rate (Brodribb 2009, Scoffoni et al. 2016). However, water has to be channeled from the soil to the canopy via the xylem (Petit and Hampe 2006). Indeed, the links between stem xylem structure, hydraulics and tree growth have been demonstrated by numerous studies (Enquist et al. 1999, Tyree and Zimmermann 2002, Zhang and Cao 2009, Fan et al. 2012), and tradeoffs between fundamental functions, such as xylem hydraulic conductivity ($K_s$), storage capacity and embolism resistance, have been frequently reported (Gleason et al. 2016, Pratt and Jacobsen 2016, Chen et al. 2020, S.-B. Zhang et al., 2022b). Therefore, these three xylem hydraulic traits must be balanced according to the growing environment's requirements to ensure a species' survival, growth and overall competitiveness (Lebrija-Trejos et al. 2010).

Xylem functional traits and strategies vary across species, phylogeny and habitats (Scholz et al. 2007, Feild and Wilson 2012, Janssen et al. 2020, Laughlin et al. 2020), and tree growth depends on the interaction between multiple functional

†These authors contributed equally to this work.

traits (Lebrija-Trejos et al. 2010, Rowland et al. 2021). For instance, large vessel diameter, low wood density (WD) and high $K_s$ are often associated with rapid tree growth (Enquist et al. 1999, Fan et al. 2012, Eller et al. 2018). However, a 20-year rainfall exclusion experiment showed that water limitations may alter general trait–growth relationships (Rowland et al. 2021). Therefore, trees growing in a habitat under atypical conditions require special adaptation.

Karsts cover a large fraction of the southwestern region of China, and environmental conditions in karsts differ from those in any other habitat (Chen et al. 2010). Specifically, karsts are formed by carbonate deposits that have undergone millions of years of erosion leaving behind rocky skeletons covered with thin and isolated soil layers (Geekiyanage et al. 2019). In these environments, the soil is typically poor in nutrients and water storage is limited despite sufficient precipitation, because most rainwater runs off or infiltrates through rock cavities (J. Zhang et al., 2022a). Nevertheless, trees growing in this habitat form a forest with a unique composition and structure (Nie et al. 2019). The differences in functional traits and floristic composition between karst and non-karst forests suggest strong environmental filtering in karst forests (Fu et al. 2019, Nie et al. 2019, Zhang et al. 2021). Therefore, peculiar trait–growth relationships are expected to occur in karst forests.

From a xylem hydraulic perspective, three hypotheses related to fast and sustained resource transport can tentatively explain how xylem hydraulic efficiency, safety and water storage, which are three major aspects of plant hydraulics, may promote tree growth in karst habitats. (i) High xylem hydraulic efficiency is hypothesized to promote fast resource transport, thereby supporting high photosynthetic rate (Brodribb 2009) and consequently, allowing rapid growth rate. (ii) High xylem hydraulic safety is hypothesized to sustain water transport even under low water availability (Li et al. 2009), thus, resulting in a high cumulative growth rate. (iii) Under low water availability, high-water storage is hypothesized to buffer the xylem tension to maintain the integrity of highly efficient but fragile conduits, thereby allowing transpiration extending photosynthetic active period during water stress (Chapotin et al. 2006, Scholz et al. 2007). Thus, high-water storage may also support high cumulated photosynthesis, and thus a high growth rate. If a tradeoff exists between hydraulic efficiency, safety and water storage in karst tree species as in species from other habitats (Pratt and Jacobsen 2016), then species combining high hydraulic efficiency, safety and storage, and synchronized correlations of high hydraulic efficiency, safety and storage with high growth rate, are less likely. A study on early angiosperms showed that xylem parenchyma may alter these tradeoffs (Aritsara et al. 2021). Therefore, these tradeoffs have to be tested before analyzing the contribution of these three hydraulic features to tree growth of karst species.

Owing to strong environmental filtering in karst habitats, the adaptation strategy adopted by tree species in these habitats may affect their growth. The occurrence of both deciduous and evergreen species in Chinese karst habitats (Du et al. 2017) suggests the coexistence of different growth strategies. Compared with evergreen species, deciduous species generally exhibit higher photosynthetic activity when resources are abundant; thus, they adopt a fast resource-acquisition strategy, which also coordinates with xylem structure and hydraulic functions (Choat et al. 2005, Qi et al. 2021). Deciduous species perform well in habitats with stronger seasonality (Givnish 2002). Thus, leaf habit potentially modifies the relationship between xylem hydraulic traits and tree growth in karst habitats.

Additionally, the metabolic theory of ecology proposes a general scaling between tree size and growth (Enquist et al. 1999, Muller-Landau et al. 2006). Understory trees have limited light resources and are exposed to low evaporative demand. Contrastingly, large trees have access to a relatively deeper water reservoir and a larger soil volume to uptake water; however, water has to be transported over a longer distance (Petit and Hampe 2006). Large trees also have a large canopy and are constantly exposed to higher irradiations and stronger winds (Anten and Schieving 2010, Meinzer et al. 2011). Additionally, energy and biomass costs related to aging, reproduction and respiration increase as the tree grows (Spicer and Holbrook 2007, Meinzer et al. 2011). The constraints on growth and trait–growth relationships change accordingly. Therefore, the hydraulic basis of the scaling relationship between tree size and growth needs to be clarified.

This study aimed to identify the contribution of vessel and parenchyma structure to xylem hydraulic traits and, subsequently, tree growth in a subtropical karst forest. We hypothesized that the association of large vessels with paratracheal parenchyma alters the hydraulic tradeoffs, and improves the xylem hydraulic efficiency, safety and water storage of karst species. Our second hypothesis was that the coordinated improvement of these three aspects of xylem hydraulics promotes rapid tree growth and modulates growth–size scaling relationships in karst species.

## Materials and methods

### *Study site and plant materials*

This study was performed in the Mulun National Nature Reserve (25°9′9″ N, 108°2′23″ E, 420 m elevation; Figure 1), where relatively well-preserved subtropical evergreen–deciduous mixed forests grow in a karstic formation. Based on a 2018 survey, these forests contain 879 trees per hectare—with a diameter at breast height (DBH) larger than 5 cm. The total basal area is 12.5 $m^2$ per hectare, and the dominant height (the average height of the 100 largest trees) is 10.9 m

an elliptical disk with an elliptical central hole representing the pith.

During dehydration, deciduous species, such as *R. sinica*, were completely shed their leaves before the water potential reached $P_{88}$. Thus, their vulnerability curve was constructed as far beyond $P_{50}$ as water potential and flow rate were accurately measured. The average $K_{max}$ of branches with a water potential between −0.5 and 0 MPa was used to represent the species $K_s$. The other leafy branches were left on the ground to dry. Before subsequent measurements, they were covered with a plastic bag to equilibrate the water potential. Later, the percentage loss of conductivity (PLC) was calculated using Eqn. (5) as follows:

$$PLC = \frac{K_{max} - K_D}{K_{max}} \times 100 \quad (5)$$

The vulnerability curves were fitted to a double-parameter Weibull function using the *fitplc* R-package, which allows the estimation of the water potential at 50% loss of conductivity ($P_{50}$) for each species (Duursma and Choat 2017). $P_{50}$ represents the xylem embolism resistance.

### *Wood density, saturated water content and xylem anatomy*

Five 10-cm-long segments from five distinct individuals were cut from the segment used for $K_s$ measurements. The segments were located ~1 m from the tip to avoid errors due to vessel tapering (Olson and Rosell 2013). Half of the segment was used for xylem anatomy measurements, and the other half for WD and saturated water content (SWC) measurements.

The portion dedicated to wood anatomy was stored in a formalin–alcohol–acetic acid fixation solution (10:50:5:distilled water 35; Ruzin 1999) and processed within 2 months. Before sectioning, a polystyrene and ethyl acetate solution was used to prevent tissue deformation (Barbosa et al. 2010). Subsequently, 25-$\mu$m thick sections were cut using a sliding microtome (Leica SM2010 R, Nusslock, Germany). Sections were stained with safranin and Alcian blue and then mounted on Canadian balsam (Figure 1c). Images were captured using a light microscope (Leica DM 3000 LED; Wetzlar, Germany). Xylem tissues were manually identified in each image and delimited using a modified polyline tool in ImageJ (Figure 1d) and a drawing pad (BOSTO 16HDK, Guangdong, China). The diameter $d_i$ of each vessel $i$ was calculated from its area assuming a circular shape, and the mean hydraulically weighted diameter ($Dh$) of each individual was calculated as per Eq. (6) (Tyree and Zimmermann 2002):

$$Dh = \frac{1}{n}\sqrt[4]{\sum_{i=1}^{n} d_i^4} \quad (6)$$

The relative area occupied by each tissue on the cross-section represented the tissue fraction. In addition, vessel connectivity with xylem tissue was analyzed following Aritsara et al. (2021). Briefly, this analysis determined the relative length of the vessel perimeter in direct contact with other xylem tissues; that is, vessel–vessel connectivity, vessel–axial parenchyma connectivity (VAP), vessel–ray connectivity, vessel–fiber connectivity (*VFc*) and vessel–tracheid connectivity. The last parameter only applied to the two species with apparent vasicentric tracheids (identified from longitudinal sections).

The segment dedicated to *WD* and *SWC* measurements was debarked, and the pith was removed. The sample was immersed in distilled water for 24 h. Then, the saturated mass was weighted on a scale with $10^{-4}$ resolution (MT204T, Shanghai, China). The saturated volume ($V_{sat}$) was measured on the same instrument using the liquid displacement principle (Perez-Harguindeguy et al. 2013). The sample was oven-dried for >72 h at 70 °C, and the dry mass (*DM*) was measured. *WD* is the ratio of *DM* to $V_{sat}$, and *SWC* is the saturated water weight relative to *DM*.

### *Statistical analysis*

All statistical analyses and illustrations were conducted using R.3.5.3 (R Core Team 2019). Trait correlations were calculated using the *smatr* R-package (Warton et al. 2012). Principal component analysis (PCA) was performed based on four structural and three hydraulic traits using the *prcomp* function. For the PCA, the missing hydraulic trait values of *M. integerrimum* and *T. rotundifolia* were interpolated using the *missMDA* package. Structural equation model (SEM) analysis was used to analyze the interdependent relationships between xylem structure and hydraulics. Multiple SEMs were then computed using the *sem* function of the *lavaan* R-package (Rosseel 2012), and the best model was selected based on *RMSEA* and *AIC* values.

## Results

Across the studied species, xylem $K_s$, SWC and $P_{50}$ varied by 1.7-, 21.9- and 5.4-fold, respectively. Xylem embolism resistance ranged from −1.10 MPa (*Sinosideroxylon pedunculatum*) to −6.99 MPa (*Boniodendron minus*) (Figure S1 available as Supplementary data at *Tree Physiology* Online).

### *Structural and hydraulic trait differences between evergreen and deciduous species*

In the multivariate space of PCA, deciduous and evergreen species were distinguished into two groups (Figure 2). *T*-test comparison of principal component scores between the two groups (*P*-value of PC1: 0.056, PC2: 0.031) showed that deciduous species were dominant in the upper left region of the PCA, which was characterized by high VAP and *SWC* but low *WD*. Comparative tests showed that deciduous species differed from evergreen species only in *Dh*, *SWC* and WD, with deciduous species showing higher *Dh* than that of evergreen ones

Table 1. Description of the 22 studied species by leaf habit.

| Species | Family | Life form | MVL (cm) | DBH 2018 (cm) | IVI 2018 |
|---|---|---|---|---|---|
| DECIDUOUS | | | | | |
| *Boniodendron minus* | Sapindaceae | Tree | 68.6 | 12.4 ± 0.3 | 1.35 |
| *Chukrasia tabularis* | Meliaceae | Tree | 41.6 | 12 ± 1.4 | 3.62 |
| *Cipadessa baccifera* | Meliaceae | Dwarf tree | 67.5 | 7.9 ± 1.1 | 1.03 |
| *Croton lachynocarpus* | Euphorbiaceae | Dwarf tree | 44.5 | 8.4 ± 0.3 | 3.16 |
| *Eurycorymbus cavaleriei* | Sapindaceae | Tree | 33.2 | 10.6 ± 0.6 | 1.03 |
| *Pteroceltis tatarinowii* | Cannabaceae | Tree | 115 | 15.6 ± 0.6 | 16.91 |
| *Triadica rotundifolia* | Euphorbiaceae | Tree | 56 | 15.8 ± 4.2 | 0.56 |
| EVERGREEN | | | | | |
| *Bridelia balansae* | Phyllanthaceae | Tree | 64 | 13.6 ± 1 | 0.68 |
| *Callicarpa macrophylla* | Lamiaceae | Dwarf tree | 59.4 | 6.5 ± 0.4 | 0.77 |
| *Canthium dicoccum* | Rubiaceae | Tree | 34.6 | 9.2 ± 1.1 | 1.22 |
| *Cleidion bracteosum* | Euphorbiaceae | Dwarf tree | 17.3 | 7.3 ± 0.3 | 0.17 |
| *Cryptocarya calcicola* | Lauraceae | Tree | 26.1 | 8.1 ± 0.4 | Outside the plot |
| *Cyclobalanopsis glauca* | Fagaceae | Tree | 114 | 10.9 ± 1.2 | 1.44 |
| *Decaspermum gracilentum* | Myrtaceae | Dwarf tree | 96.5 | 5.4 ± 0.2 | 1.17 |
| *Ficus glaberrima* | Moraceae | Tree | 13.2 | 19.5 ± 3.4 | 1.2 |
| *Glycosmis pentaphylla* | Rutaceae | Dwarf tree | 29 | 6.4 ± 0.3 | 2.39 |
| *Litsea salicifolia* | Lauraceae | Tree | 11.7 | 7.6 ± 0.8 | 0.78 |
| *Micromelum integerrimum* | Rutaceae | Dwarf tree | 77 | 6.2 ± 1.1 | 0.7 |
| *Murraya paniculata* | Rutaceae | Dwarf tree | 47.4 | 6.4 ± 0.1 | 4.13 |
| *Myrsine kwangsiensis* | Primulaceae | Tree | 61.4 | 7.6 ± 0.3 | 4.73 |
| *Radermachera sinica* | Bignoniaceae | Tree | 90 | 13.5 ± 0.5 | 4.17 |
| *Sinosideroxylon pedunculatum* | Sapotaceae | Tree | 61.5 | 8.8 ± 0.4 | 4.1 |

*Micromelum integerrimum*, for which we only found three individuals and collected data from one for conservation purposes. Thus, hydraulic traits and growth information were missing for this species. Additionally, the secretion of viscous latex prevented accurate measurements of the hydraulic traits of *Triadica rotundifolia*. Maximum vessel length (MVL) was measured using the air injection method (Greenidge 1952), and the results are shown in Table 1. Branches at least twice as long as MVL were cut from the canopy with a 15 m extendable pruner, except for *P. tatarinowii* and *Cyclobalanopsis glauca*, from which branches longer than MVL were collected. The basal end of the branch was wrapped in a wet paper towel and tightly banded with a wrap film to prevent dehydration. The branches were double wrapped in black plastic bags and light-colored gunny bags from outside to prevent transpiration, overheating and mechanical damage during transportation to the laboratory, which was accomplished within 1 h.

The bench-top drying method was used to induce embolism in the branches, and a flowmeter (Bronkhorst 5 g/h, Ruurlo, The Netherlands) was used to measure the flow. Upon arrival at the improvised laboratory, several leaves were wrapped in aluminium zip-lock bags to equilibrate their water potential with that of the stem. They were used to monitor and measure the xylem water potential. One bagged leaf was excised, and its water potential was measured using a pressure chamber (PMS 1505 D-EXP, Corvallis, OR, USA). The measured water potential was double-checked against that of another leaf to ensure homogeneity within the branch. Leafless branch segments were selected, ensuring that they remained longer than MVL after successive trimming. Furthermore, the segments were trimmed by ~2 cm from both ends underwater, and were immersed for at least 30 min to release xylem tension. Tension release was repeated at least twice. The segments were trimmed again at both ends. Subsequently, the basal end was shaved using a sharp cutter blade, connected directly to the flowmeter with a head pressure of ~3 kPa (Espino and Schenk 2011) corresponding to a water denivelation of 30 cm, and the native flow rate ($F_0$) was recorded when the flow rate measurement stabilized. Native embolism was flushed using a degassed 10-mM KCl aqueous solution at 150–250 kPa for at least 30 min. Then, the maximum flow rate ($F_{max}$) was measured using the flowmeter. Native and maximum $K_s$ ($K_0$ and $K_{max}$, respectively) were calculated using the following equation (Melcher et al. 2012):

$$K = \frac{F \cdot L}{\Delta P \cdot A_w} \quad (4)$$

where $F$ is the measured flow, $L$ is the length of the segment, $\Delta P$ is the hydrostatic pressure difference between the sample and the water level in the reservoir and $A_w$ is the sapwood area at the middle of the segment. $A_w$ was assumed as the area of

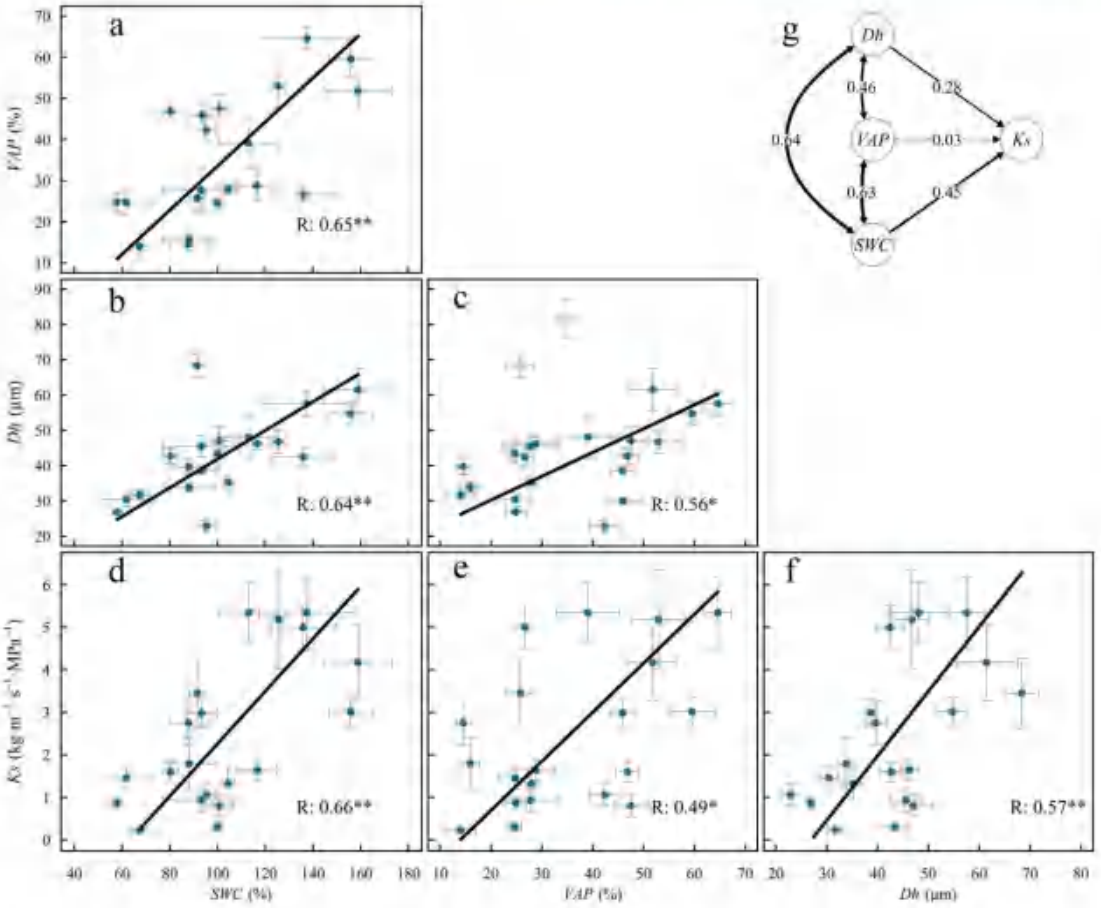


Figure 3. Relationships between xylem anatomical traits and hydraulic traits, vessel hydraulically weighted mean diameter (*Dh*), VAP, *SWC* and $K_S$. The structural equation model (b) evidences the complexity of the relationships. Each path of the SEM model was separately represented by a reduced major axis correlation and shown in panels (a–f). Points drawn in gray (*C. glauca* and *T. rotundifolia*) on the (c) panel are outliers. From panels (d–f), *M. integerrimum* and *T. rotundifolia* have xylem structural trait values but no $K_S$ data. Each point represents the species average, and error bars are the standard errors. *: $0.05 > P > 0.01$, **: $0.01 > P > 0.001$.

within a range for which high vessel density can compensate. In addition, the thick vessel walls of the deciduous species may have compensated for the potential vulnerability of their wide vessels. The resulting similarity in terms of xylem $K_S$ and embolism resistance between the two groups of species suggests that xylem structure converged toward the adaptation of karst species to water deficit and nutrient availability limitations, thereby explaining the coexistence of both groups.

### *Xylem water storage and anatomy are associated with $K_S$ but not with embolism resistance*

Our regression analysis revealed intercorrelations between VAP, *Dh*, *SWC* and $K_S$, such that paratracheal parenchyma, large vessels and high capacity for water storage ensured a high-water transport rate through the xylem in karst tree species. This result is consistent with theories and functional relationships reported by various studies on species from different environments (Tyree and Zimmermann 2002, Morris et al. 2018, Janssen et al. 2020, Áritsara et al. 2021). For instance, the relationship between $K_S$ and *Dh* is theoretically linked to the Hagen–Poiseuille equation wherein xylem $K_S$ is proportional to the fourth power of the xylem vessel diameter (Tyree and Zimmermann 2002). In turn, the xylem parenchyma-paratracheal arrangement, that is, high VAP is associated with large vessels (Morris et al. 2018) and high $K_S$ (Áritsara et al. 2021). In addition, species with high *SWC* have been frequently reported to show high capacitance (Ziemińska et al. 2020), which helps to maintain the integrity of large vessels having high $K_S$ (Meinzer et al. 2003). Large-diameter vessels can transport water faster but are often vulnerable to hydraulic dysfunction (Sperry et al. 2006). To prevent vessel dysfunction, plants

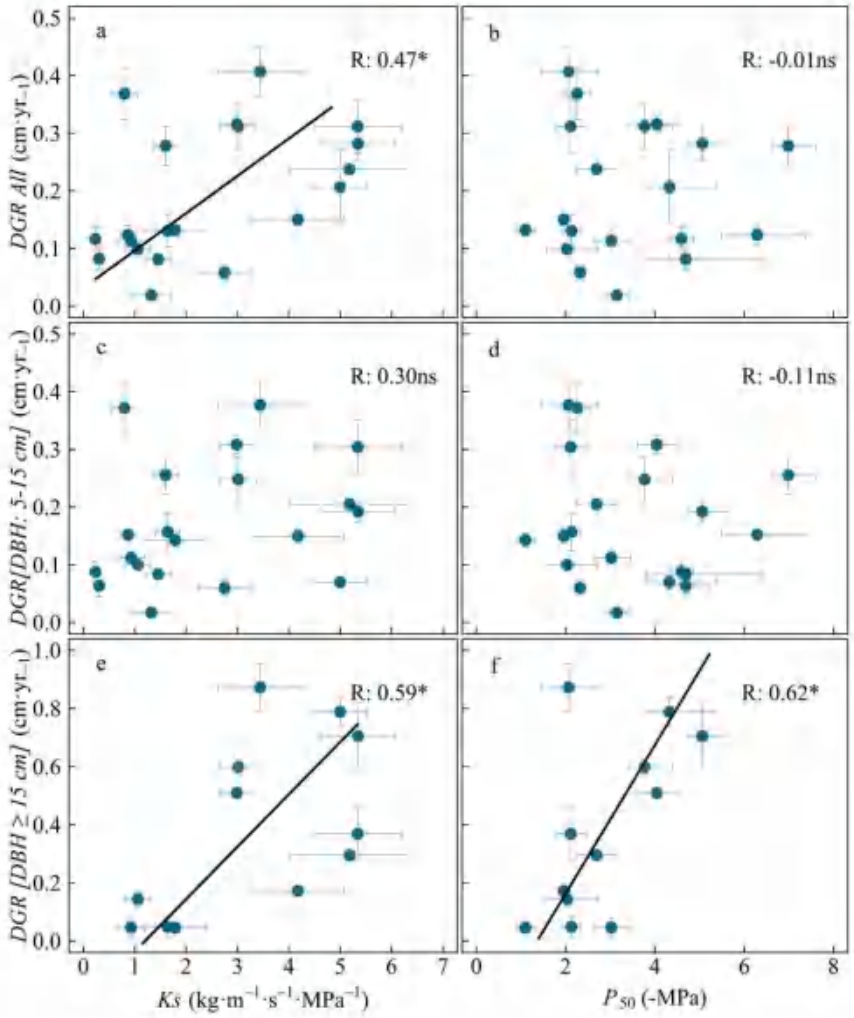


Figure 4. Contributions of xylem $K_s$ and embolism resistance ($P_{50}$) to the average *DGR* at species level within two diameter ranges. *Micromelum integerrimum* and *T. ratundifolia* have no data on $K_s$ and $P_{50}$. Thus, 20 species were shown in panels (a–d); in panels (e–f), only 12 species had individuals exceeding 15 cm *DBH*. Each point represents the species average; error bars are the standard errors. *: $0.05 > P > 0.01$, 'ns': $P > 0.1$.

can mobilize stored water to buffer the xylem water potential and delay embolism initiation (Scholz et al. 2007, McCulloh et al. 2019). However, this buffering mechanism also depends on the xylem parenchyma structure (Vesala 2003, Ziemińska et al. 2020). Specifically, xylem parenchyma cells channel water from storage tissues to vessels (Zwieniecki and Holbrook 2009, Brodersen et al. 2010), and relatively strong connectivity between xylem parenchyma and vessels facilitates this exchange (James et al. 2003, Zwieniecki and Holbrook 2009). In karst habitats, when soil water supply decreases, storage water in plants may either (i) temporarily supplement the transpiration stream, thereby maintaining photosynthesis and producing additional biomass, or (ii) maintain the vessels in a functional state, such that they can be readily operational as soon as soil water becomes available again. The second mechanism seems most likely because transpiration can be rapidly halted when fine roots sense a water deficit (Carminati et al. 2020, Rodriguez-Dominguez and Brodribb 2020). The independence of $P_{50}$ to the studied anatomical traits can be associated with the strong correlation between $P_{50}$ and inter-vessel pit structure (Levionnois et al. 2021), but the structural compensation discussed above warrants further investigation of such a relationship among karst species. Therefore, vessel dimension, parenchyma arrangement and water storage of karst tree species support xylem hydraulic efficiency.

### *Xylem hydraulic efficiency and safety promoted tree diameter growth in karst habitats*

We observed that the tree species that achieved relatively high $K_s$ grew faster than those with lower $K_s$. This finding

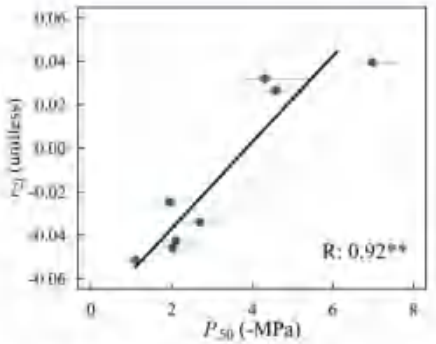


Figure 5. Contribution of embolism resistance ($P_{50}$) to growth acceleration ($r_{2i}$) with increasing tree size based on the growth model proposed by Iida et al. (2014). Only nine of the 22 species had significant size–growth scaling relationships, the correlation for all species is in supporting information Figure S3 available as Supplementary data at *Tree Physiology* Online. Data show the species average, and the error bars of $P_{50}$ are the range between the 0.025 and 0.975 quantiles from the bootstraps of the vulnerability curve. No error bar was computed for $r_{2i}$ and $stDGR_{15}$. **: $0.01 > P > 0.001$.

is consistent with the positive correlation observed previously between theoretical xylem conductivity and growth rate in tropical seasonal rainforests (Fan et al. 2012). Species with high hydraulic efficiency can transport large amounts of water within a short period. The ephemeral water availability after rainfall in karst habitat (Fu et al. 2016) may explain why trees with high hydraulic efficiency grow faster than trees with low efficiency. Overall, the positive correlation between $K_s$ and *DGR* was stronger than that between absolute $P_{50}$ and *DGR*, and the latter correlation became positive and significant in trees with *DBH* above 15 cm. These two correlations suggest that species with relatively high hydraulic conductance and high embolism resistance grew faster. The results also indicated that the correlations between hydraulic traits and tree growth were stronger than the correlations between anatomical traits and growth of karst tree species. This is consistent with the findings in a seasonal tropical forests where traits directly associated with water transport and photosynthesis had stronger correlation with tree growth than more commonly measured traits (Rowland et al. 2021).

In terms of safety, the observed positive correlation between absolute $P_{50}$ and tree growth in large trees contradicts tradeoffs or non-significant relationships reported by other studies (Hajek et al. 2014, Ahmad et al. 2018, Eller et al. 2018, Rowland et al. 2021). The importance of embolism resistance for tree growth in karst habitat can be an adaptation to the shallow root layer leading to intermittent water availability (Fu et al. 2016). Indeed, a water and biomass model on seasonal dry tropical forests showed that some trees lost their leaves quickly after intermittent rainfall (Xu et al. 2016), probably due to low hydraulic safety, thus, limiting tree growth. The positive correlation between absolute $P_{50}$ and tree growth in large trees, emphasized by that between absolute $P_{50}$ and standardized growth rate at 15 cm *DBH*, coincides with the exposure of large trees to the high-water tension at the canopy level (Hamlyn 1992). Thus, the need for fast and safe water transport at the canopy overrides the effect of light and carbon assimilation on the growth of trees growing under water-deficit conditions (Muller-Landau et al. 2006, Rowland et al. 2021).

Within the last decade, several researchers have integrated plant hydraulic traits into biosphere models and predicted with more or less accuracy water and carbon budget at plant, ecosystem and regional scales (Christoffersen et al. 2016, Xu et al. 2016, Mencuccini et al. 2019). The empirical correlation of hydraulic efficiency and safety with tree growth observed in this study will allow us to select and calibrate models that better fit karst environments. Nevertheless, tree growth is a complex mechanism, and realistic models should not disregard whole-plant trait coordination, macro- and microclimate, and biotic interactions between cohabiting organisms. Overall, our results illustrate the importance of fast and safe water transport for tree growth on karst formations, which may explain the lack of tradeoff between hydraulic efficiency and safety.

### *Greater cavitation resistance is correlated with higher growth acceleration with increasing DBH*

Absolute $P_{50}$ was strongly and positively correlated with the slope $r_{2i}$, i.e. growth acceleration, based on the growth–size relationship model of Iida et al. (2014). Two mechanisms are proposed to explain the relationship between $P_{50}$ and tree growth acceleration. (i) Iida et al. (2014) partly attributed the decreasing growth rate with increasing stem diameter with the accumulation of dead wood. Reciprocally, physiological traits that extend sapwood lifespan may reverse this trend. Indeed, sapwood with high embolism resistance could have a longer lifespan as emboli shorten the vessel lifespan (Jacobsen et al. 2018). Thus, the resulting increase in functional sapwood area may be consistent with the increasing growth rate with increasing stem diameter. (ii) Species with high embolism resistance are compromised by slower growth at an early age; as trees of these species grow taller, they acquire greater access to light and water (deeper rooting) resources, which in turn facilitate faster growth (Meinzer et al. 2011, Gleason et al. 2018). The correlation between more negative $P_{50}$ and high growth acceleration potentially integrate mechanism such as xylem lifespan, resource acquisition and forest succession. Our results highlighted that embolism resistance modulates tree growth dynamics in karst habitats, but clarifying the related physiological mechanisms requires further investigations.

## Conclusion

Our results demonstrated structured relationships linking xylem anatomy, hydraulics and tree growth rate and dynamics in a

Rosseel Y (2012) Lavaan: an R package for structural equation modeling. J Stat Softw 48:1–36.
Rowland L, Oliveira RS, Bittencourt PRL et al. (2021) Plant traits controlling growth change in response to a drier climate. New Phytol 229:1363–1374.
Ruzin SE (1999) Plant microtechnique and microscopy. Oxford University Press, New York.
Scholz FG, Bucci SJ, Goldstein G, Meinzer FC, Franco AC, Miralles-Wilhelm F (2007) Biophysical properties and functional significance of stem water storage tissues in Neotropical savanna trees. Plant Cell Environ 30:236–248.
Scoffoni C, Chatelet DS, Pasquet-kok J, Rawls M, Donoghue MJ, Edwards EJ, Sack L (2016) Hydraulic basis for the evolution of photosynthetic productivity. Nat Plants 2:16072. https://doi.org/10.1038/nplants.2016.72.
Sperry JS, Hacke UG, Pittermann J (2006) Size and function in conifer tracheids and angiosperm vessels. Am J Bot 93:1490–1500.
Spicer R, Holbrook NM (2007) Parenchyma cell respiration and survival in secondary xylem: does metabolic activity decline with cell age? Plant Cell Environ 30:934–943.
Tyree MT, Zimmermann MH (2002) Xylem structure and the ascent of sap. Springer, Berlin, Heidelberg.
Vallet P, Perot T (2016) Tree diversity effect on dominant height in temperate forest. For Ecol Manage 381:106–114.
Vesala T (2003) Refilling of a hydraulically isolated embolized xylem vessel: model calculations. Ann Bot 91:419–428.
Warton DI, Duursma RA, Falster DS, Taskinen S (2012) Smatr 3- an R package for estimation and inference about allometric lines: the smatr 3- an R package. Methods Ecol Evol 3:257–259.
Xu X, Medvigy D, Powers JS, Becknell JM, Guan K (2016) Diversity in plant hydraulic traits explains seasonal and inter-annual variations of vegetation dynamics in seasonally dry tropical forests. New Phytol 212:80–95.
Zanne AE, Westoby M, Falster DS, Ackerly DD, Loarie SR, Arnold SEJ, Coomes DA (2010) Angiosperm wood structure: global patterns in vessel anatomy and their relation to wood density and potential conductivity. Am J Bot 97:207–215.
Zhang J, Chen H, Fu Z, Luo Z, Wang F, Wang K (2022) Effect of soil thickness on rainfall infiltration and runoff generation from karst hillslopes during rainstorms. Eur J Soil Sci 73:e13288.
Zhang JL, Cao KF (2009) Stem hydraulics mediates leaf water status, carbon gain, nutrient use efficiencies and plant growth rates across dipterocarp species. Funct Ecol 23:658–667.
Zhang QW, Zhu SD, Jansen S, Cao KF (2021) Topography strongly affects drought stress and xylem embolism resistance in woody plants from a karst forest in Southwest China. Funct Ecol 35:566–577.
Zhang S-B, Wen G-J, Qu Y-Y, Yang L-Y, Song Y (2022) Trade-offs between xylem hydraulic efficiency and mechanical strength in Chinese evergreen and deciduous savanna species. Tree Physiol 42:1337–1349.
Zhao YT, Ali A, Yan ER (2016) The plant economics spectrum is structured by leaf habits and growth forms across subtropical species. Tree Physiol 37:173–185.
Ziemińska K, Rosa E, Gleason SM, Holbrook NM (2020) Wood day capacitance is related to water content, wood density, and anatomy across 30 temperate tree species. Plant Cell Environ 43:3048–3067.
Zwieniecki MA, Holbrook NM (2009) Confronting Maxwell's demon: biophysics of xylem embolism repair. Trends Plant Sci 14:530–534.

karst habitat. The xylem structure alone is hardly related to tree growth unless the hydraulic efficiency and safety determined by this structure are considered. For instance, large vessels, high-water storage and paratracheal xylem parenchyma promoted hydraulic efficiency. Moreover, there was no significant tradeoff between hydraulic efficiency and safety, and both promoted tree diameter growth. In addition, stronger xylem embolism resistance was linked to higher growth acceleration with increasing tree size. Furthermore, our results highlight that, in addition to hydraulic efficiency, hydraulic safety significantly influences the growth of karst trees, particularly that of large trees. The close association between water regime and tree growth rate and dynamics in karst forests demonstrates a high sensitivity of karst habitats to climatic disorders, influencing forest production and mortality, and consequently, the carbon sequestration efficiency of the ecosystem. Therefore, we strongly recommend the direct integration of empirically measured hydraulic traits into models aiming to analyze actual and future primary production and carbon stock distribution, particularly in regions with abundant karst ecosystems.

## Acknowledgments

We express our sincere gratitude to the managers of the Mulun Protected Area for allowing us to perform the study on-site, and to the students from the Plant Ecophysiology and Evolution group for their contribution to the measurement of annual growth. We are thankful to the Editor and the anonymous reviewers for their contribution to the improvement of the manuscript.

## Supplementary data

Supplementary data for this article are available at *Tree Physiology* Online.

## Conflict of interest

None declared.

## Funding

S.-D.Z. was supported by the National Natural Science Foundation of China (32060330), the Natural Science Foundation of Guangxi Zhuang Autonomous Region (2018GXNSFAA294027) and the Bagui Young Scholarship of Guangxi Zhuang Autonomous Region. A.N.A.A. was supported by the China Postdoctoral Fellowship Council.

## Authors' contributions

A.N.A.A. and M.-Y.N. contributed equally to the trait measurements, data analysis and preparation of the manuscript. A.N.A.A, S.-D.Z and K.-F.C worked on the experimental design and wrote the manuscript. W.-H.Z, C.-L.Y and H.-Q.S contributed to hydraulic empirical measurements. Y.-Q.W performed the measurements of tree growth.

## Data and materials availability

The data related to this article are publicly available from figshare through the doi: 10.6084/m9.figshare.22208782.

## References

Ahmad HB, Lens F, Capdeville G, Burlett R, Lamarque LJ, Delzon S (2018) Intraspecific variation in embolism resistance and stem anatomy across four sunflower (*Helianthus annuus* L.) accessions. Physiol Plant 163:59–72.

Anten NPR, Schieving F (2010) The role of wood mass density and mechanical constraints in the economy of tree architecture. Am Nat 175:250–260.

Aritsara ANA, Razakandraibe VM, Ramananantoandro T, Gleason SM, Cao KF (2021) Increasing axial parenchyma fraction in the Malagasy Magnoliids facilitated the co-optimisation of hydraulic efficiency and safety. New Phytol 229:1467–1480.

Barbosa ACF, Pace MR, Witovisk L, Angyalossy V (2010) A new method to obtain good anatomical slides of heterogeneous plant parts. IAWA J 31:373–383.

Brodersen CR, McElrone AJ, Choat B, Matthews MA, Shackel KA (2010) The dynamics of embolism repair in xylem: in vivo visualizations using high-resolution computed tomography. Plant Physiol 154:1088–1095.

Brodribb TJ (2009) Xylem hydraulic physiology: the functional backbone of terrestrial plant productivity. Plant Sci 177:245–251.

Carminati A, Ahmed MA, Zarebanadkouki M, Cai G, Lovric G, Javaux M (2020) Stomatal closure prevents the drop in soil water potential around roots. New Phytol 226:1541–1543.

Chapotin SM, Razanameharizaka JH, Holbrook NM (2006) Water relations of baobab trees (*Adansonia* spp. L.) during the rainy season: does stem water buffer daily water deficits? Plant Cell Environ 29:1021–1032.

Chen HS, Zhang W, Wang KL, Fu W (2010) Soil moisture dynamics under different land uses on karst hillslope in Northwest Guangxi, China. Environ Earth Sci 61:1105–1111.

Chen ZC, Zhu SD, Zhang YT, Luan JW, Li S, Sun PS, Wan X, Liu S (2020) Tradeoff between storage capacity and embolism resistance in the xylem of temperate broadleaf tree species. Tree Physiol 40:1029–1042.

Choat B, Ball MC, Luly JG, Holtum JAM (2005) Hydraulic architecture of deciduous and evergreen dry rainforest tree species from North-Eastern Australia. Trees 19:305–311.

Christoffersen BO, Gloor M, Fauset S et al. (2016) Linking hydraulic traits to tropical forest function in a size-structured and trait-driven model (TFS v.1-hydro). Geosci Model Dev 9:4227–4255.

Cottam G, Curtis JT (1956) The use of distance measures in phytosociological sampling. Ecology 37:451–460.

Du H, Hu F, Zeng F, Wang K, Peng W, Zhang H, Zeng Z, Zhang F, Song T (2017) Spatial distribution of tree species in evergreen-deciduous broadleaf karst forests in Southwest China. Sci Rep 7:15664.

Duursma R, Choat B (2017) Fitplc – an R package to fit hydraulic vulnerability curves. J Plant Hydraul 4:1–14.

Eller CB, Barros FdV, Bittencourt PRL, Rowland L, Mencuccini M, Oliveira R (2018) Xylem hydraulic safety and construction costs

determine tropical tree growth: tree growth vs hydraulic safety trade-off. Plant Cell Environ 41:548–562.

Enquist BJ, West GB, Charnov EL, Brown JH (1999) Allometric scaling of production and life-history variation in vascular plants. Nature 401:907–911.

Espino S, Schenk HJ (2011) Mind the bubbles: achieving stable measurements of maximum hydraulic conductivity through woody plant samples. J Exp Bot 62:1119–1132.

Fan ZX, Zhang SB, Hao GY, Ferry Slik JW, Cao KF (2012) Hydraulic conductivity traits predict growth rates and adult stature of 40 Asian tropical tree species better than wood density. J Ecol 100: 732–741.

Feild T, Wilson JP (2012) Evolutionary voyage of angiosperm vessel structure-function and its significance for early angiosperm success. Int J Plant Sci 173:596–609.

Fu PL, Zhu SD, Zhang JL, Finnegan PM, Jiang YJ, Lin H, Fan ZX, Cao KF (2019) The contrasting leaf functional traits between a karst forest and a nearby non-karst forest in south-West China. Funct Plant Biol 46:907–915.

Fu TD, Chen HS, Fu ZY, Wang KL (2016) Surface soil water content and its controlling factors in a small karst catchment. Environ Earth Sci 75:1406.

Geekiyanage N, Goodale U, Cao KF, Kitajima K (2019) Plant ecology of tropical and subtropical karst ecosystems. Biotropica 51:626–640.

Givnish T (2002) Adaptive significance of evergreen vs. deciduous leaves: solving the triple paradox. Silva Fenn 36:703–743.

Gleason SM, Westoby M, Jansen S et al. (2016) Weak tradeoff between xylem safety and xylem-specific hydraulic efficiency across the world's woody plant species. New Phytol 209:123–136.

Gleason SM, Stephens AEA, Tozer WC et al. (2018) Shoot growth of woody trees and shrubs is predicted by maximum plant height and associated traits. Funct Ecol 32:247–259.

Greenidge KNH (1952) An approach to the study of vessel length in hardwood species. Am J Bot 39:570–574.

Hajek P, Leuschner C, Hertel D, Delzon S, Schuldt B (2014) Trade-offs between xylem hydraulic properties, wood anatomy and yield in Populus. Tree Physiol 34:744–756.

Hamlyn GJ (1992) Plants and microclimate. Cambridge University Press, UK.

Iida Y, Poorter L, Sterck F, Kassim AR, Potts MD, Kubo T, Kohyama TS (2014) Linking size-dependent growth and mortality with architectural traits across 145 co-occurring tropical tree species. Ecology 95:353–363.

Jacobsen AL, Valdovinos-Ayala J, Pratt RB (2018) Functional lifespans of xylem vessels: development, hydraulic function, and post-function of vessels in several species of woody plants. Am J Bot 105: 142–150.

James S, Meinzer F, Goldstein G, Woodruff D, Jones T, Restom T, Mejia M, Clearwater M, Campanello P (2003) Axial and radial water transport and internal water storage in tropical forest canopy trees. Oecologia 134:37–45.

Janssen TAJ, Höltta T, Fleischer K, Naudts K, Dolman AH (2020) Wood allocation trade-offs between fiber wall, fiber lumen and axial parenchyma drive drought resistance in neotropical trees. Plant Cell Environ 43:965–980.

Laughlin DC, Delzon S, Clearwater MJ, Bellingham PJ, McGlone MS, Richardson SJ (2020) Climatic limits of temperate rain-forest tree species are explained by xylem embolism resistance among angiosperms but not among conifers. New Phytol 226: 727–740.

Lebrija-Trejos E, Pérez-García EA, Meave JA, Bongers F, Poorter L (2010) Functional traits and environmental filtering drive community assembly in a species-rich tropical system. Ecology 91: 386–398.

Levionnois S, Jansen S, Wandji RT et al. (2021) Linking drought-induced xylem embolism resistance to wood anatomical traits in Neotropical trees. New Phytol 229:1453–1466.

Li Y, Sperry JS, Shao M (2009) Hydraulic conductance and vulnerability to cavitation in corn (*Zea mays* L.) hybrids of differing drought resistance. Environ 66:341–346.

Lu M, Du H, Song T et al. (2021) Drivers of tree survival in an evergreen-deciduous broadleaf karst forest in Southwest China. For Ecol Manage 499:119598.

McCulloh KA, Domec J, Johnson DM, Smith DD, Meinzer FC (2019) A dynamic yet vulnerable pipeline: integration and coordination of hydraulic traits across whole plants. Plant Cell Environ 42:2789–2807.

Meinzer F, James SA, Goldstein G, Woodruff D (2003) Whole-tree water transport scales with sapwood capacitance in tropical forest canopy trees. Plant Cell Environ 26:1147–1155.

Meinzer FC, Lachenbruch B, Dawson TE (eds) (2011) Size- and age-related changes in tree structure and function. Springer, Dordrecht, The Netherlands.

Melcher PJ, Holbrook NM, Burns MJ, Zwieniecki MA, Cobb AR, Brodribb TJ, Choat B, Sack L (2012) Measurements of stem xylem hydraulic conductivity in the laboratory and field. Methods Ecol Evol 3:685–694.

Mencuccini M, Manzoni S, Christoffersen B (2019) Modelling water fluxes in plants: from tissues to biosphere. New Phytol 222: 1207–1222.

Méndez-Alonzo R, Paz H, Zuluaga RC, Rosell JA, Olson ME (2012) Coordinated evolution of leaf and stem economics in tropical dry forest trees. Ecology 93:2397–2406.

Morris H, Gillingham MAF, Plavcová L et al. (2018) Vessel diameter is related to amount and spatial arrangement of axial parenchyma in woody angiosperms. Plant Cell Environ 41:245–260.

Muller-Landau HC, Condit RS, Chave J et al. (2006) Testing metabolic ecology theory for allometric scaling of tree size, growth and mortality in tropical forests. Ecol Letters 9:575–588.

Nie YP, Ding YL, Zhang HL, Chen HS (2019) Comparison of woody species composition between rocky outcrops and nearby matrix vegetation on degraded karst hillslopes of Southwest China. J For Res 30:911–920.

Olson ME, Rosell JA (2013) Vessel diameter-stem diameter scaling across woody angiosperms and the ecological causes of xylem vessel diameter variation. New Phytol 197:1204–1213.

Perez-Harguindeguy N, Diaz S, Garnier E et al. (2013) New handbook for standardised measurement of plant functional traits worldwide. Aust J Bot 61:167–234.

Petit RJ, Hampe A (2006) Some evolutionary consequences of being a tree. Annu Rev Ecol Evol Syst 37:187–214.

Pratt RB, Jacobsen AL (2016) Conflicting demands on angiosperm xylem: Tradeoffs among storage, transport and biomechanics. Plant Cell Environ 40:1–17.

Qi J-H, Fan Z-X, Fu P-L, Zhang Y-J, Sterck F (2021) Differential determinants of growth rates in subtropical evergreen and deciduous juvenile trees: carbon gain, hydraulics and nutrient-use efficiencies. Tree Physiol 41:12–23.

R Core Team (2019) R: A language and environment for statistical computing. R Foundation for Statistical Computing, Austria.

Rennolls K (1978) 'Top height'; its definition and estimation. Commonw For Rev 57:215–219.

Rita A, Pericolo O, Saracino A, Borghetti M (2020) Sperry's packing rule affects the spatial proximity but not clustering of xylem conduits: the case of *Fagus sylvatica* L. IAWA J 42:1–20.

Rodriguez-Dominguez CM, Brodribb TJ (2020) Declining root water transport drives stomatal closure in olive under moderate water stress. New Phytol 225:126–134.

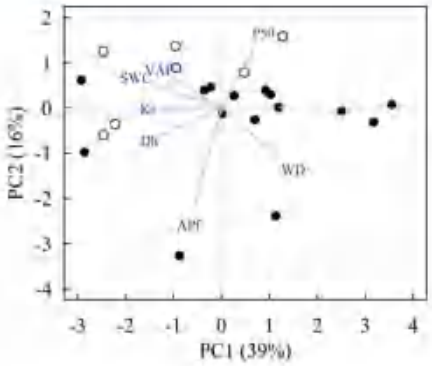


Figure 2. Principal component analysis synthesizing the relationships between xylem anatomy and hydraulic across 22 karst species. Each point represents the species average. Deciduous and evergreen species are shown in open and filled points, respectively. *Dh*: vessel hydraulically weighted mean diameter, *SWC*: xylem saturated water content, *WD*: sapwood density, $K_s$: sapwood specific hydraulic conductivity, $P_{50}$: xylem water potential at 50% loss conductivity, *APF*: axial parenchyma fraction.

(Table S1 available as Supplementary data at *Tree Physiology* Online).

### *Relationships between xylem structure, hydraulic function and tree growth rate*

No significant tradeoff has been observed between $K_s$, *SWC* and $P_{50}$ (Figure S2 available as Supplementary data at *Tree Physiology* Online). Among all studied structural traits, *Dh*, *VAP*, *VFc* and *WD* showed the strongest correlations with $K_s$ and *SWC*, but none of the studied anatomical features was significantly correlated with $P_{50}$ (Figure 2). Because VAP and *VFc* exhibited a strong negative correlation due to spatial complementarity ($R^2$ = 0.52, $P$ < 0.001), only one of the two, that is, VAP, was integrated into the analysis of xylem structure–hydraulic relationships. Furthermore, regression analysis showed significant positive correlations between *Dh*, VAP, *SWC* and $K_s$ (Figure 3), suggesting strong interactions between vessel dimensions, parenchyma structure, water storage and $K_s$. Based on SEM, the direct path coefficient between VAP and $K_s$ was weaker than indirect paths via the contributions of VAP to *Dh* and *SWC*, and then to $K_s$. $P_{50}$ was excluded from SEM due to the lack of correlation with the other traits (Figure 3g).

None of the traits that significantly distinguished evergreen from deciduous species directly correlated with diameter growth rate (DGR) (Table S1 and Figure S2 available as Supplementary data at *Tree Physiology* Online). Regardless of the tree diameter classes, average *DGR* was positively correlated with $K_s$ but not with *SWC* or $P_{50}$ (Figure 4a and b, Figure S2 available as Supplementary data at *Tree Physiology* Online). Among trees with *DBH* ranging from 5 to 15 cm, $K_s$ and $P_{50}$ were not significantly correlated with *DGR* (Figure 4 c and d). Furthermore, among trees with *DBH* exceeding 15 cm, both $K_s$ and absolute $P_{50}$ were positively correlated with *DGR* (Figure 4e and f).

### *Relationships between hydraulic functions and tree growth dynamics*

Based on the growth–size relationship model of Iida et al. (2014), only 8 of the 22 species showed a significant size-dependent growth rate (Table S2 available as Supplementary data at *Tree Physiology* Online). Slope factor, $r_{2i}$, was strongly and positively correlated with absolute $P_{50}$ across the species with significant size-dependent growth (Figure 5). The relationship remained significant when the other species were added to the analysis (Figure S3a available as Supplementary data at *Tree Physiology* Online). Additionally, the absolute value of $P_{50}$ was positively correlated with the tree growth standardized for 15 cm *DBH* trees (Figure S3b available as Supplementary data at *Tree Physiology* Online).

## Discussion

Our results revealed that xylem hydraulic efficiency increased with xylem vessel diameter, paratracheal parenchyma arrangement and water storage in subtropical karst tree species. Furthermore, xylem hydraulic efficiency and embolism resistance promoted fast tree growth in large trees. Moreover, xylem embolism resistance was related to increasing growth acceleration as tree diameter increased.

### *Difference in structure and similarity in hydraulic traits between evergreen and deciduous tree species*

Our comparative analyses showed that the branch xylem of evergreen and deciduous tree species significantly differed in WD and vessel diameter (Figure 2, Table S1 available as Supplementary data at *Tree Physiology* Online). The significantly low WD of deciduous species, compared with evergreen species, was consistent with previous reports (Méndez-Alonzo et al. 2012, Zhao et al. 2016). Evergreen species tended to compensate for their narrower vessels with marginally higher vessel density to achieve a hydraulic efficiency similar to that of deciduous species (Table S1 available as Supplementary data at *Tree Physiology* Online). It is important to emphasize that this kind of compensation may not suffice in non-karst habitats because it has been shown that deciduous species have significantly higher $K_s$ values than evergreen species in savanna and tropical seasonal dry forests (Choat et al. 2005, S.-B. Zhang et al., 2022). In fact, vessel packing limitation rule governs a one-power tradeoff between vessel diameter and density (Zanne et al. 2010, Rita et al. 2020), and vessel diameter has four-power effects on hydraulic efficiency (Tyree and Zimmermann 2002). Nevertheless, in karst habitats, the need for hydraulic safety may entail limited vessel expansion in deciduous species. Thus, vessel diameter was maintained

8、 硕士研究生阶段成绩单

广西大学硕士研究生成绩单

| 学号 | 1809301019 | 姓名 | | 倪鸣源 | 培养层次 | 学术硕士 | 学位分 |
|---|---|---|---|---|---|---|---|
| 学院 | 林学院 | 学科专业 | | 生态学 | 总学分 | 32 | 16 |
| 序号 | 课程名称 | 课程类别 | 学分 | 学时 | 考试类别 | 成绩 | 任课老师 |
| 1 | 生态学专题 | 学位课 | 3.0 | 48 | 正考 | 83 | 招礼军 |
| 2 | 生物多样性专题 | 学位课 | 2.0 | 32 | 正考 | 89 | 赖家业 |
| 3 | 生态学研究法 | 学位课 | 2.0 | 32 | 正考 | 79 | 温远光 |
| 4 | 生物统计与数据分析 | 学位课 | 2.0 | 32 | 正考 | 81 | 覃林 |
| 5 | 中国特色社会主义理论与实践研究 | 学位课 | 2.0 | 32 | 正考 | 95 | 张锐 |
| 6 | 自然辩证法概论 | 学位课 | 1.0 | 16 | 正考 | 86 | 严建新 |
| 7 | 英语(硕士) | 学位课 | 4.0 | 64 | 正考 | 88 | 辜贤禹 |
| 8 | 土壤理化分析 | 非学位课 | 2.0 | 32 | 正考 | 83 | 招礼军 |
| 9 | 高级植物生理学 | 非学位课 | 2.0 | 32 | 正考 | 91 | 朱师丹 |
| 10 | 生态影响评价 | 非学位课 | 2.0 | 32 | 正考 | 64 | 谢伟东 |
| 11 | 植物分类学 | 非学位课 | 2.0 | 32 | 正考 | 86 | 罗应华 |
| 12 | 森林资源监测与评价 | 非学位课 | 2.0 | 32 | 正考 | 65 | 李春干 |
| 13 | 社会实践 | 社会实践 | 2.0 | | 正考 | 通过 | |
| 14 | 学术活动 | 学术活动 | 2.0 | | 正考 | 通过 | |
| 15 | 开题报告 | 开题报告 | 2.0 | | 正考 | 通过 | |

经办人 陶世凡

学院公章 西大 林学院

研究生院公章

打印时间：2020/10/21 10:44:10

备注：该成绩单需同时有广西大学研究生成绩管理专用章和学院章才生效

第 19 页 共 49 页